



Tuning alpha rhythms to shape conscious visual perception / Di Gregorio F.; Trajkovic J.; Roperti C.; Marcantoni E.; Di Luzio P.; Avenanti A.; Thut G.; Romei V. In: CURRENT BIOLOGY. ISSN 0960-9822. - STAMPA. - 32:5(2022), pp. 988-998. [10.1016/j.cub.2022.01.003]

ALMA MATER STUDIORUM
UNIVERSITÀ DI BOLOGNA

ARCHIVIO ISTITUZIONALE
DELLA RICERCA

Alma Mater Studiorum Università di Bologna Archivio istituzionale della ricerca

Tuning alpha rhythms to shape conscious visual perception

This is the final peer-reviewed author's accepted manuscript (postprint) of the following publication:

Published Version:

Availability:

This version is available at: <https://hdl.handle.net/11585/879206> since: 2022-03-22

Published:

DOI: <http://doi.org/10.1016/j.cub.2022.01.003>

Terms of use:

Some rights reserved. The terms and conditions for the reuse of this version of the manuscript are specified in the publishing policy. For all terms of use and more information see the publisher's website.

This item was downloaded from IRIS Università di Bologna (<https://cris.unibo.it/>).
When citing, please refer to the published version.

(Article begins on next page)

This is the final peer-reviewed accepted manuscript of:

Di Gregorio, F., Trajkovic, J., Roperti, C., Marcantoni, E., Di Luzio, P., Avenanti, A., Thut, G., & Romei, V. (2022). Tuning alpha rhythms to shape conscious visual perception. *Current Biology*, 32(5), 988-998.e6.

The final published version is available online at: <https://doi.org/10.1016/j.cub.2022.01.003>

Rights / License:

The terms and conditions for the reuse of this version of the manuscript are specified in the publishing policy. For all terms of use and more information see the publisher's website.

This item was downloaded from IRIS Università di Bologna (<https://cris.unibo.it/>)

When citing, please refer to the published version.

ARTICLE TITLE: **Tuning alpha rhythms to shape conscious visual perception**

1

2 **Article type:** Article

3

Authors: Francesco Di Gregorio^{1*}, Jelena Trajkovic^{2*}, Cristina Roperti²,
Eleonora Marcantoni², Paolo Di Luzio², Alessio Avenanti^{2,3}, Gregor Thut⁴, Vincenzo
Romei^{2,5}

4

5 **Journal:** Current Biology

6

7 **Funding:** V.R. is supported by BIAL foundation (204/18).

8

9 DOI: [10.1016/j.cub.2022.01.003](https://doi.org/10.1016/j.cub.2022.01.003)

10

11

12

13

Tuning alpha rhythms to shape conscious visual perception

Francesco Di Gregorio^{1*}, Jelena Trajkovic^{2*}, Cristina Roperti², Eleonora Marcantoni², Paolo Di Luzio², Alessio Avenanti^{2,3}, Gregor Thut⁴, Vincenzo Romei^{2,5}

¹ UO Medicina riabilitativa e neuroriabilitazione, Azienda Unità Sanitaria Locale, via Castiglione 29, 40139, Bologna, Italy;

² Centro studi e ricerche in Neuroscienze Cognitive, Dipartimento di Psicologia, Alma Mater Studiorum – Università di Bologna, Campus di Cesena, via Pavese 50, 47521, Cesena, Italy;

³ Centro de Investigación en Neuropsicología y Neurociencias Cognitivas, Universidad Católica del Maule, Av San Miguel, 346000, Talca, Chile;

⁴ Centre for Cognitive Neuroimaging, School of Psychology and Neuroscience, University of Glasgow, 56-64 Hillhead Street, G12 8QB, Glasgow, UK;

⁵ IRCCS Fondazione Santa Lucia, Via Ardeatina, 306/354, 00179, Roma, Italy.

*Equally contributed

Corresponding author and Lead Contact: mail to vincenzo.romei@unibo.it (VR)
Centro studi e ricerche in Neuroscienze Cognitive, Dipartimento di Psicologia, Alma Mater Studiorum – Università di Bologna, Campus di Cesena, 47521 Cesena, Italy
Twitter Handle: @VincenzoRomei

Summary

It is commonly held that what we see and what we believe we see are overlapping phenomena. However, dissociations between sensory events and their subjective interpretation occur in the general population and in clinical disorders, raising the question as to whether perceptual accuracy and its subjective interpretation represent mechanistically dissociable events. Here, we uncover the role that alpha oscillations play in shaping these two indices of human conscious experience. We used electroencephalography (EEG) to measure occipital alpha oscillations during a visual detection task, which were then entrained using rhythmic-TMS. We found that controlling pre-stimulus alpha-frequency by rhythmic-TMS modulated perceptual accuracy but not subjective confidence in it, while controlling post-stimulus (but not pre-stimulus) alpha-amplitude modulated how well subjective confidence judgments can distinguish between correct and incorrect decision, but not accuracy. These findings provide the first causal evidence of a double-dissociation between alpha-speed and -amplitude, linking alpha-frequency to spatio-temporal sampling resources, and alpha-amplitude to the internal, subjective representation and interpretation of sensory events.

Keywords: Conscious Perception, Alpha Oscillations, Alpha Amplitude, Alpha Frequency, Visual Perception, Confidence, Rhythmic Transcranial Magnetic Stimulation, Alpha Entrainment.

14 **Introduction**

15 The well-known axiom “Seeing is believing” implies that what we see and what
16 we *believe* we see are largely overlapping phenomena. However, there are many
17 examples of dissociations between sensory events and their subjective
18 interpretation, both in the general population (i.e. false memories^{1,2}) and in
19 subclinical^{3,4} and clinical psychiatric populations (e.g. schizophrenia⁵). A key
20 question, therefore, is whether perceptual accuracy and its subjective interpretation
21 represent mechanistically dissociable events of our conscious experience. And, if so,
22 what their neural underpinnings might be.

23 Alpha oscillations (range 7-13Hz) in the human brain may play an active role in
24 both sensory processing and conscious perception⁶⁻¹⁵. In particular, pre-stimulus
25 alpha-amplitude has been shown to account for a momentary level of cortical
26 excitability¹⁶ and to predict subjective confidence in response to visual stimuli¹⁷⁻¹⁹.
27 Specifically, higher levels of alpha-amplitude seem to account for reduced subjective
28 confidence and reduced proneness to reporting a visual percept (more conservative
29 decision criterion), without affecting the level of accuracy of the response²⁰. These
30 new insights into the role of alpha-amplitude in perception suggest that alpha-
31 amplitude might not primarily reflect perceptual accuracy, but rather a change in the
32 internal response criterion. However, this leaves open a fundamental question: what
33 are the oscillatory correlates of perceptual accuracy?

34 Recent reports have highlighted the relevance of alpha-frequency in perceptual
35 sampling, with faster alpha oscillations resulting in higher temporal resolution and
36 more accurate perceptual experience²¹⁻²⁷, potentially through an increased
37 accumulation of sensory evidence over time. Importantly, we hypothesize here that
38 this higher temporal resolution of visual sampling can successfully translate into

39 higher accuracy in general, by allocating more resources to the perceptually relevant
40 sensory dimension within the same amount of time.

41 Here, in a first experiment, we have used a visual detection task with spatially
42 lateralized stimuli and electroencephalography (EEG), to directly test the hypotheses
43 that (1) alpha-frequency accounts for objective accuracy (correct vs. erroneous
44 responses and d' measures²⁸), while (2) alpha-amplitude predicts subjective
45 confidence (low vs. high confidence responses) and/or (3) relates to meta-cognitive
46 abilities, i.e. how well subjective confidence judgments can distinguish between
47 correct and incorrect decisions (as indexed by meta- d' measures²⁹).

48 Crucially, in a second experiment, we used rhythmic Transcranial Magnetic
49 Stimulation (rhythmic-TMS) prior to stimulus onset around individual alpha-frequency
50 (IAF) to entrain pre-stimulus oscillatory activity in the alpha-band towards slower or
51 faster alpha-frequency or higher alpha-amplitudes, in order to influence individual
52 performance towards lower or higher accuracy or to impact individual subjective
53 confidence levels, respectively.

54 Finally, as stimulus processing has been shown to influence metacognitive
55 abilities³⁰⁻³², in a third experiment, we delivered rhythmic-TMS at each participant's
56 own IAF post-stimulus but prior to a subjective confidence prompt to test how
57 increases in post-stimulus alpha-amplitude can modulate their ability to distinguish
58 between correct and incorrect decisions, measured by means of meta- d' .

59

Results

60 A total of 92 participants took part in three experiments (Figure 1), designed to map
61 pre-stimulus alpha-frequency and alpha-amplitude on objective versus subjective

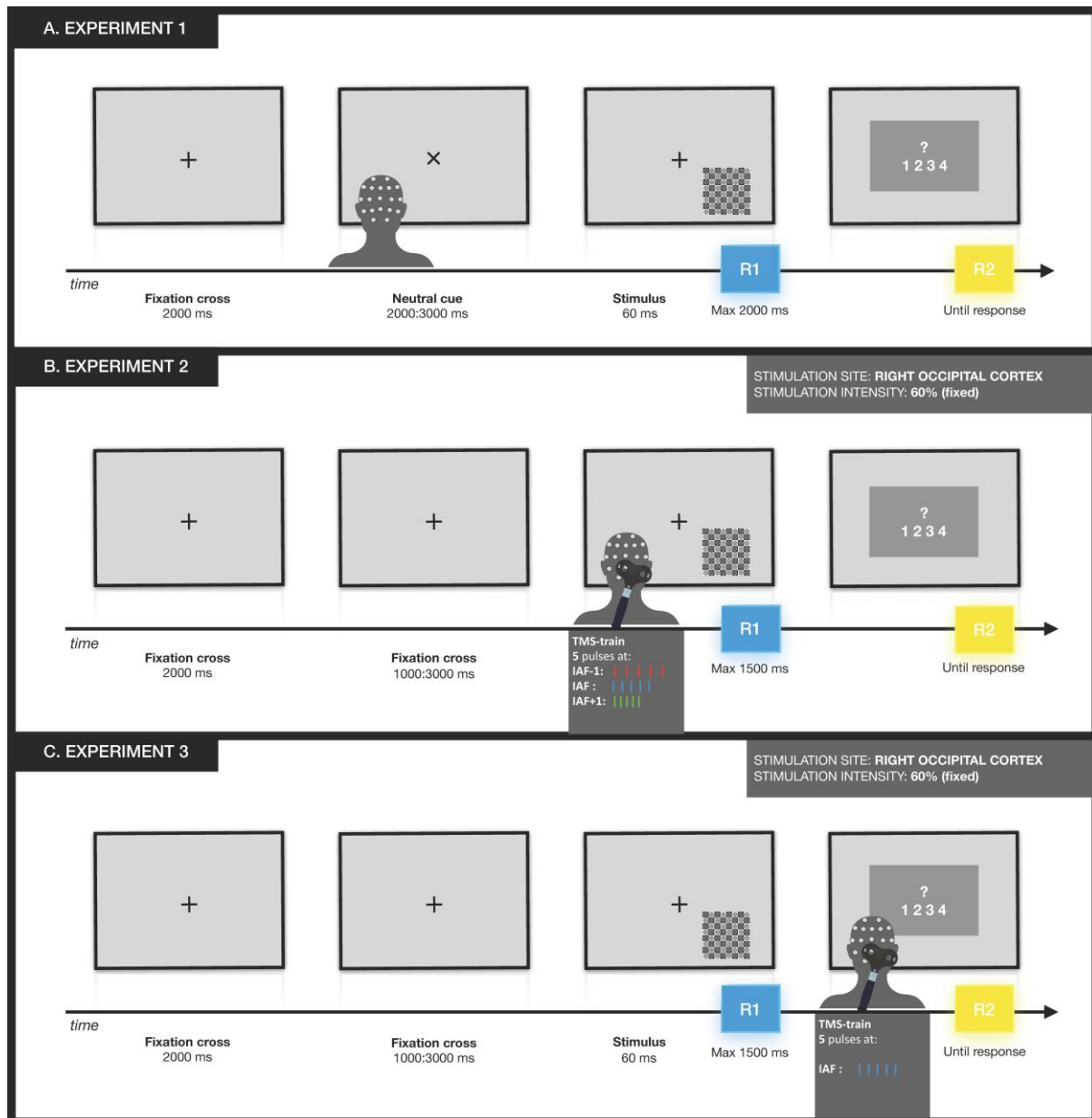
62 performance measures (EEG Experiment 1) and to test for their causative
63 relationships (TMS-EEG Experiments 2&3).

64

65 **Alpha-frequency and alpha-amplitude dissociate with respect to objective**
66 **accuracy, subjective confidence and metacognitive abilities**

67 In Experiment 1, twenty-four participants (12 women; mean age=23.2,
68 SE=2.61) performed a visual detection task (Figure 1A) in which lateralized stimuli
69 (8X8 checkerboards) were preceded by a spatially uninformative cue (an X),
70 indicating that a stimulus will be occurring in the lower left- or right-hemifield with
71 50% probability (chance level). Each black and white checkerboard was flashed for
72 60ms and could contain iso-luminant grey circles, the contrast of which was set for
73 each individual to their 50% perceptual threshold. Half of the trials were catch trials,
74 i.e. checkerboards without any grey circle embedded in them (see Methods for
75 details).

76 Participants were instructed to respond whenever they perceived grey circles
77 within the lateralized checkerboards. Following this primary task and about 1.5-2sec
78 post-stimulus, they were prompted to indicate on a scale of 1 to 4 how confident they
79 were of their percept, with 1 representing “no confidence at all”, 2, “little confidence”,
80 3 “moderate confidence” and 4 “high confidence” (see Figure 1A). EEG signals were
81 concurrently recorded from 64 electrodes while this task was performed (see
82 Methods).



83

84 **Figure 1. Experimental design.** A. Experiment 1: EEG data were collected
 85 during a visual detection task. Each trial started with a fixation cross, after which
 86 stimuli could randomly appear in the lower left or right visual field. The primary task
 87 was to respond (R1) by pressing a space bar if the checkerboard contained grey
 88 circles. After this, participants rated their confidence in their first response (R2) on a
 89 Likert scale from 1 (no confidence at all) to 4 (high confidence). B. Experiment 2:
 90 Participants performed the same visual detection task as in Experiment 1 while
 91 undergoing concurrent EEG recording. In addition, 5 rhythmic-TMS pulses were
 92 administered before stimulus presentation. Participants were assigned to 3 different
 93 groups. For each group, rhythmic-TMS pulses were set at a certain alpha-frequency:
 94 individual alpha-frequency (IAF) group (blues bars), slower pace (IAF-1Hz) group
 95 (red bars), and faster pace (IAF+1Hz) group (green bars). C. Experiment 3:
 96 Participants performed the same visual detection task while undergoing EEG
 97 recordings, as in Experiments 1 and 2. However, rhythmic-TMS pulses were
 98 administered before the confidence prompt at each participant's individual alpha-
 99 frequency. ms=milliseconds.

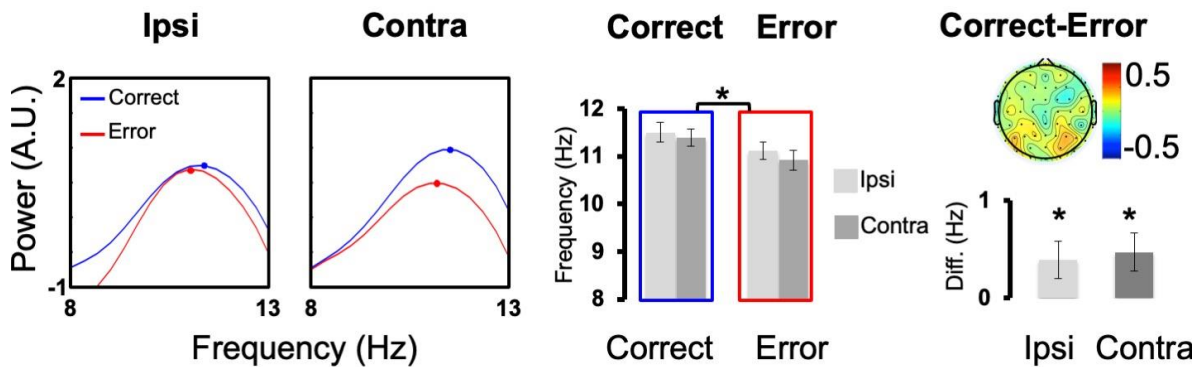
100

101 *Pre-stimulus alpha-frequency and accuracy:* We looked at whether correct vs.
102 erroneous responses could be best explained by the frequency of alpha oscillations
103 prior to stimulus presentation, rather than by their amplitude. Our analysis of pre-
104 stimulus alpha-frequency (Figure 2A) showed a significant main effect of
105 ACCURACY (Correct vs. Errors) ($F(1,23)=18.2$, $p<.001$, $\eta_p^2=.442$). This result
106 suggests that individual pre-stimulus alpha-frequency can differentiate between
107 correct and erroneous responses, with faster alpha-frequency predicting correct
108 responses ($M=11.45\text{Hz}$, $SE=0.18\text{Hz}$) and slower alpha-frequency predicting errors
109 ($M=11.02\text{Hz}$, $SE=0.18\text{ Hz}$). Moreover, the effect of alpha-frequency was maximal
110 over the posterior electrodes (Figure 2A, map inset), involving left and right sites
111 equally, as no main effect of HEMISPHERE (ipsilateral vs. contralateral to the
112 presented stimulus) ($F(1,23)=1.34$, $p=.259$, $\eta_p^2=.06$), nor a significant interaction of
113 ACCURACYxHEMISPHERE ($F(1,23)=0.33$, $p=.571$, $\eta_p^2=.014$) were found.

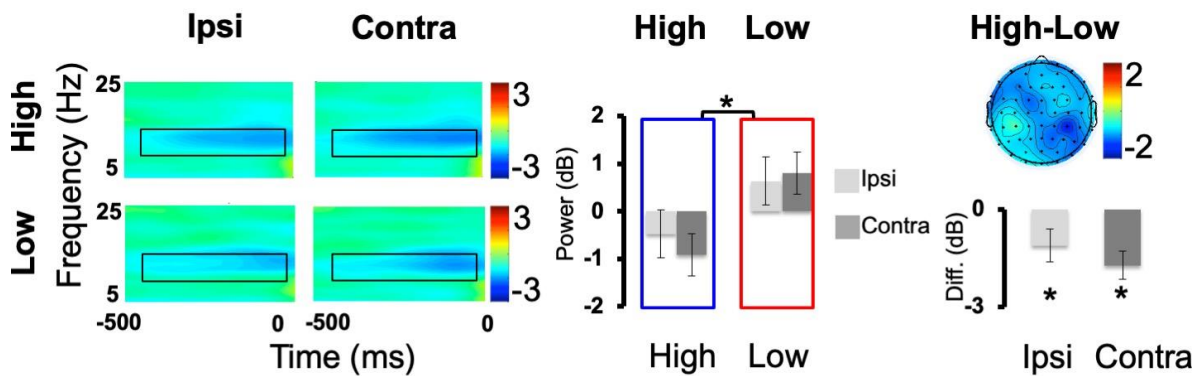
114 We further tested whether pre-stimulus alpha-frequency can predict individual
115 performance across participants as assessed by d' , a sensitivity index that takes into
116 account both correct responses and false alarms, and thus – relative to the simple hit
117 rate measure – has the advantage of discounting any potential effect of response
118 bias, with higher values reflecting higher task accuracy²⁸. Using a median split
119 procedure for d' scores, we divided participants in two numerically equivalent groups
120 (high vs low d'). In line with our hypothesis, a between-groups analysis of alpha-
121 frequency show faster pre-stimulus alpha-frequency in the high d' group (11.55Hz ,
122 $SE=0.22\text{Hz}$) compared to the low d' group (10.29Hz , $SE=0.66\text{Hz}$) by 1.26Hz :
123 $t(22)=1.832$, $p=.040$, $d=.374$ (one-tailed unpaired two-sample t-test).

124 By contrast, the analysis of both pre- and post-stimulus alpha-amplitude (see
 125 supplemental Figure S1B) showed no significant effects on ACCURACY (*all Fs*
 126 $(1,23) < 3.05$, *all ps* $> .094$, *all ηp^2* $< .117$), in line with recent reports that alpha-
 127 amplitude does not account for objective accuracy^{9,17,18,33}.

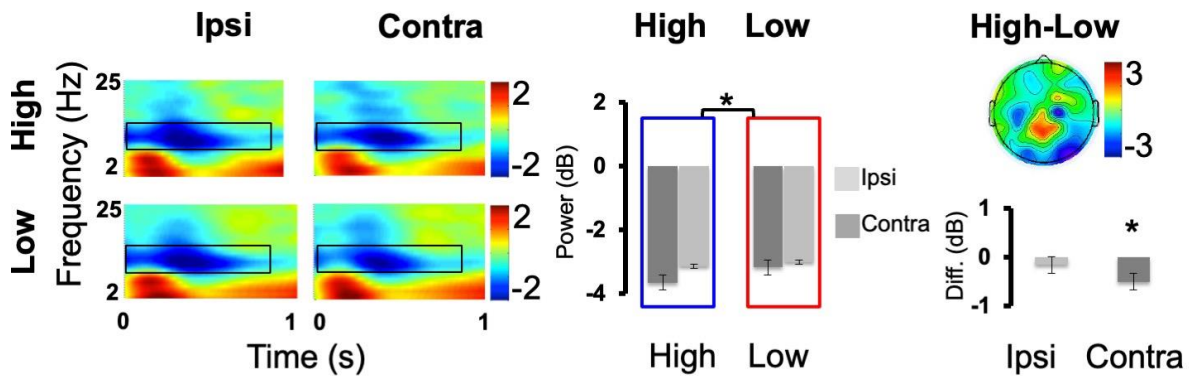
A Objective Accuracy Alpha Frequency



B Subjective Confidence Pre-stimulus Alpha Amplitude



C Post-stimulus Alpha Amplitude



128

129 **Figure 2. Results Experiment 1: Alpha-frequency and -amplitude relate to**
130 **accuracy and confidence.** A. Objective Accuracy. Averaged *alpha-frequency* is
131 represented as the z-scored mean power ($10 \cdot \log_{10}[\mu\text{V}^2/\text{Hz}]$) spectrum in the cue-
132 stimulus time period for the contralateral and the ipsilateral electrodes and for
133 Correct and Error trials within the alpha-band. Bar graphs report correct and error
134 trials and the differences in correct/error responses. Topography represents the
135 difference in Correct-Error (electrodes are flipped to represent contralateral activity in
136 the right-hand side and ipsilateral activity in the left-hand side). Subjective
137 Confidence. Pre-stimulus alpha-amplitude (B) and post-stimulus alpha-amplitude (C)
138 are reported as time-frequency plots. For illustrative purposes we reported data from
139 a cluster of ipsi (P7,PO7,PO3,O1) and contralateral (P8,PO8,PO4,O2) electrodes
140 and for Low and High confident trials. Black boxes denote regions of statistical
141 analyses (alpha-band 7-13Hz). Bar graphs are reported for Low and High confident
142 trials and for the difference in High-Low. Topography represents the difference in
143 High-Low (electrodes are flipped to have contralateral activity in the right-hand side
144 and ipsilateral activity in the left-hand side). Two-tailed t-test statistical significance is
145 reported ($*p < .05$). Error bars represent standard error of the mean. A.U.=arbitrary
146 units; Diff=difference; μV =microvolt; Hz=Hertz; ms=milliseconds; dB=decibel.
147 See also Figure S1.
148

149 *Pre-stimulus alpha-amplitude and confidence:* We then tested whether pre-
150 stimulus alpha-amplitude, rather than alpha-frequency, could account for confidence
151 judgments^{17,18,6} (Figure 2B). We found a main effect of CONFIDENCE
152 ($F(1,23)=9.03$, $p=.006$, $\eta_p^2=.282$), with desynchronized alpha-amplitude in high
153 confidence trials (-0.699dB, SE=0.409dB) and synchronized alpha-amplitude in low
154 confidence trials (0.719dB, SE=0.251dB), suggesting that alpha-amplitude has a
155 significant impact on perceptual confidence. Moreover, topography (Figure 2B, map
156 inset) shows posterior alpha-amplitude modulations with an even distribution across
157 hemispheres, indicating no main effect of HEMISPHERE (ipsilateral vs. contralateral
158 to the presented stimulus) $F(1,23)=0.201$, $p=.658$, $\eta_p^2=.009$), nor a significant
159 interaction CONFIDENCExHEMISPHERE ($F(1,23)=1.323$, $p=.262$, $\eta_p^2=.054$).

160 For completeness, control analyses performed on pre-stimulus alpha-
161 frequency (see supplemental Figure S1A) showed no main effect of CONFIDENCE,
162 nor any interaction with HEMISPHERE (all $F_s(1,23) < 0.47$, $p_s > .501$, $\eta_p^2 < .021$).

163

164 *Post-stimulus alpha-amplitude, confidence and meta-d'*: Because following
165 stimulus presentation the initial choice on decisions and confidence continue to
166 evolve^{31,32}, we asked whether subjective confidence judgments are influenced by
167 post-perceptual processes. To this aim, we analysed alpha-amplitude in a time
168 window after stimulus presentation (0-900ms), corresponding to a post-stimulus time
169 period but before the confidence prompt (Figure 2C). The analysis of post-stimulus
170 alpha-amplitude revealed a main effect of CONFIDENCE ($F(1,23)=4.367$, $p=.048$;
171 $\eta_p^2=.16$), with more desynchronized alpha-amplitude in high confidence trials (-
172 3.41dB, SE=0.38dB) compared to low confidence trials (-3.08db, SE=0.34dB).
173 Moreover, the analyses showed a main effect of HEMISPHERE ($F(1,23)=5.358$;
174 $p=.03$; $\eta_p^2=.189$) and most importantly, an interaction
175 CONFIDENCExHEMISPHERE ($F(1,23)=4.347$, $p=.048$, $\eta_p^2=.159$), showing that
176 when looking at post-stimulus alpha-amplitude, the confidence effects are accounted
177 for by the contralateral (high confidence=-3.64dB, SE=0.396dB; low confidence=-
178 3.14dB, SE=0.347dB; $t(23)=2.747$, $p=.011$; $d=.586$) but not the ipsilateral
179 hemisphere (high confidence=-3.17dB, SE=0.387dB; low confidence=-3.01dB,
180 SE=0.349dB; $t(23)=0.906$, $p=.375$, $d=.193$). These findings suggest that post-
181 stimulus alpha-amplitude has a retinotopic distribution being modulated by the
182 stimulus position. Indeed, while the relationship between confidence levels and pre-
183 stimulus alpha-amplitude can be observed for both hemispheres, only contralateral
184 alpha-amplitude accounts for individual confidence levels after stimulus presentation.

185 We then tested whether post-stimulus alpha-amplitude could specifically
186 account for metacognitive abilities. In other words, we tested how well subjective
187 confidence judgments can distinguish between correct and incorrect decisions, by
188 means of meta-d', a measure that quantifies metacognitive performance and that

189 reflects the efficacy of confidence ratings to discriminate objectively correct from
190 erroneous responses²⁹. In a between-subject design, by using a median-split
191 procedure, we divided participants with high and low metacognitive abilities. We
192 found that post-stimulus alpha-amplitude in the high meta-d' group was significantly
193 more desynchronized (-4.66dB, SE=0.59dB) relative to the low meta-d' group (-
194 3.26dB, SE=0.39dB; one-tailed unpaired two-sample t-test: $t(22)=1.966$, $p=.031$;
195 $d=.567$), thus supporting the idea that post-stimulus alpha-amplitude can predict
196 metacognitive performance. Moreover, this role seems specific for post-stimulus
197 alpha-amplitude, as pre-stimulus changes of alpha-amplitude could not account for
198 between-subject differences in metacognition ($t(22)=0.929$, $p=.181$, $d=.189$), further
199 supporting this interpretation.

200

201 Overall, these EEG results implicate alpha-frequency in the level of objective
202 accuracy with higher alpha-frequency accounting for higher accuracy, but playing no
203 role in determining one's individual perceptual confidence. Conversely, alpha-
204 amplitude is implicated in perceptual decision confidence, but has no role to play in
205 objective accuracy. In sum, these results point to a functional dissociation of the two
206 oscillatory markers, alpha-frequency and alpha-amplitude, which appear to shape
207 sensory sampling and the subjective readout of this sampling, respectively.

208

209 **Entraining faster vs. slower pre-stimulus alpha oscillations selectively** 210 **shapes objective accuracy**

211 In Experiment 2, we tested for the causal involvement of alpha-frequency and
212 alpha-amplitude in objective accuracy vs. confidence by using rhythmic-TMS to
213 entrain alpha oscillations while participants performed the same visual task as in

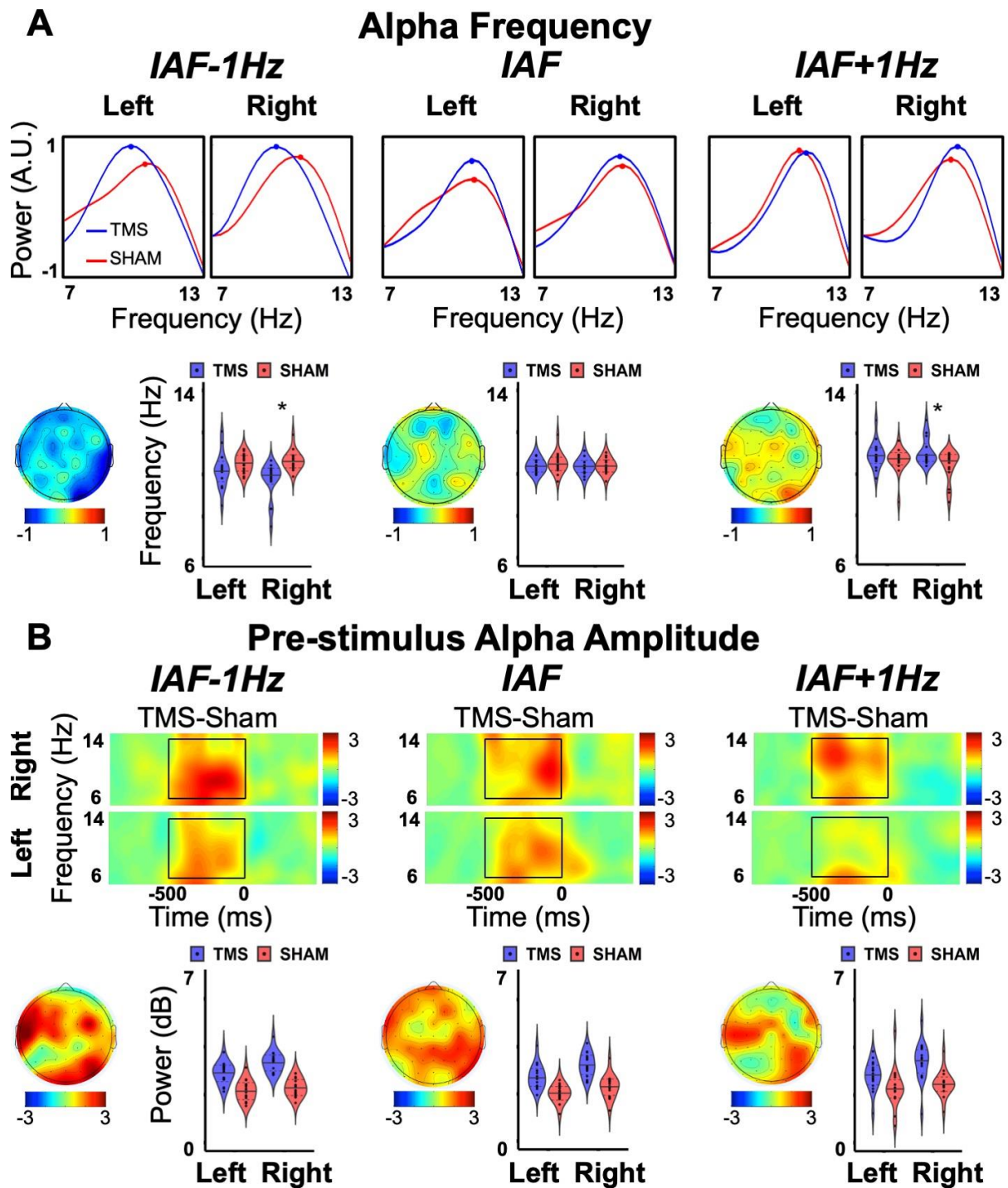
214 Experiment 1 (Figure 1B). In three different experimental groups (N=3x17
215 participants; 25 women; mean age=23.39, SE=0.36), we recorded EEG activity while
216 concurrently administering 5-pulse rhythmic-TMS trains of fixed-intensity (60% of the
217 maximum stimulator output)^{34,35} to the right occipital cortex (coil placement over O2)
218 prior to stimulus presentation. In the IAF±1Hz groups, rhythmic-TMS-frequency was
219 set at 1Hz faster/slower than the individual participant's alpha-frequency, which
220 should entrain their alpha oscillations towards a faster/slower pace^{21,22,36},
221 respectively. In the IAF group, the rhythmic-TMS frequency was aligned with the
222 participant's alpha-frequency. This has been shown to lead to enhanced alpha-
223 amplitude by entrainment^{37,38}, and should thus have an impact on confidence rather
224 than on accuracy. Together with active rhythmic-TMS, we employed sham
225 stimulation at a matching frequency for every participant in each group, to account
226 for any nonspecific effects of rhythmic-TMS.

227 Perceptual accuracy was quantified via d' score²⁸ (shown to be a more
228 sensitive measure relative to hit rates) while task confidence was estimated via
229 mean confidence and meta- d' . All measures were analysed across the two
230 hemifields (left vs. right), the two stimulation types (active rhythmic-TMS vs. sham),
231 and the three groups of participants (stimulated at IAF±1Hz and IAF).

232 We looked at the impact of rhythmic-TMS on EEG activity across the 3 groups
233 (Figure 3). As expected, pre-stimulus alpha-frequency was modulated differently in
234 active rhythmic-TMS versus sham stimulation across the experimental groups,
235 depending on the recording site (STIMULATIONxGROUPxHEMISPHERE
236 interaction: $F(2,48)=4.05$, $p=.024$, $\eta_p^2=.144$). Specifically, stimulating at the lower
237 alpha-frequency slowed down pre-stimulus alpha activity during active rhythmic-TMS
238 (M=9.74Hz, SE=0.20), relative to sham stimulation (M=10.66Hz, SE=0.20),

239 selectively at the (stimulated) right hemisphere ($t(16)=3.98$, $p=.001$, $d=.96$).
240 Conversely, stimulation at the higher alpha-frequency led to faster pre-stimulus alpha
241 activity during active rhythmic-TMS ($M=11.11\text{Hz}$, $SE=0.14$), relative to sham
242 stimulation ($M=10.43\text{Hz}$, $SE=0.31$), selectively at the stimulated site ($t(16)=2.19$,
243 $p=.043$, $d=.53$). Finally, stimulation at the exact alpha-frequency did not yield any
244 difference in the pre-stimulus alpha speed ($t(16)=0.13$, $p=.90$, $d=.03$). Moreover, we
245 found that rhythmic-TMS maximally entrained oscillatory activity exactly at the site of
246 stimulation (HEMISPHERE \times STIMULATION interaction: $F(1,48)=6.36$, $p=.015$,
247 $\eta_p^2=.117$), and at the entrained rhythm (see Figure 3A).

248 By contrast, the broadband alpha-amplitude (see Figure 3B) did not differ
249 significantly across the three groups during the entrainment protocol
250 (HEMISPHERE \times STIMULATION \times GROUP interaction: $F(2,48)=0.19$, $p=.830$,
251 $\eta_p^2=.008$). However, the entrainment effect on alpha-amplitude (quantified via the
252 difference between active rhythmic-TMS and sham stimulation) was largest at the
253 frequency of stimulation (FREQUENCY \times GROUP interaction: $F(4,96)=5.640$, $p<.001$,
254 $\eta_p^2=.19$, for details, see supplemental figure S2).



255

256

257

258

259

260

261

262

263

264

265

Figure 3. Results Experiment 2: rhythmic-TMS entrainment modulates EEG alpha-frequency and its amplitude. Results are shown for each group performing the task in Experiment 2 under different rhythmic-TMS alpha entrainment protocols (IAF±1Hz, IAF). A. (Upper) Averaged Alpha-frequency is represented as the z-scored mean power ($10 \cdot \log_{10}[\mu\text{v}^2/\text{Hz}]$) spectrum during rhythmic-TMS in the pre-stimulus time period (-650 0) in the right (stimulated) hemisphere (electrode cluster: O2,PO4,PO8) and left (non-stimulated) hemisphere (electrode cluster: O1,PO3,PO7), for active rhythmic-TMS (TMS) and SHAM-control stimulation. (Lower) Violin plots report peak frequency during TMS and SHAM for each group (IAF±1Hz, IAF) and for the left and right (stimulated) hemisphere. Data are

266 presented as median (full line) ± 1 quartile (dashed line). The topography image
267 represents the difference in alpha-frequency between TMS and SHAM stimulation.
268 B. (Upper) Pre-stimulus alpha-amplitude is presented as time-frequency plots for
269 each group (IAF ± 1 Hz, IAF) of the difference between TMS and SHAM stimulation in
270 the right (stimulated) hemisphere (electrode cluster: O2,PO4,PO8) and in the left
271 (non-stimulated) hemisphere (electrode cluster: O1,PO3,PO7). Black boxes denote
272 regions of statistical analyses (alpha-band 7-13Hz in the pre-stimulus period (-
273 500,0)). (Lower) Violin plots report alpha power during TMS and SHAM for each
274 group, and for the left and right (stimulated) hemisphere. Data are presented as
275 median (full line) ± 1 quartile (dashed line). Topography represents the difference in
276 alpha-amplitude between TMS and SHAM stimulation. Two-tailed t-test statistical
277 significance is reported (* $p < .05$). Error bars represent standard error of the mean.
278 A.U.=arbitrary units; Diff=difference; μ v=microvolt; Hz=Hertz; ms=milliseconds;
279 dB=decibel.

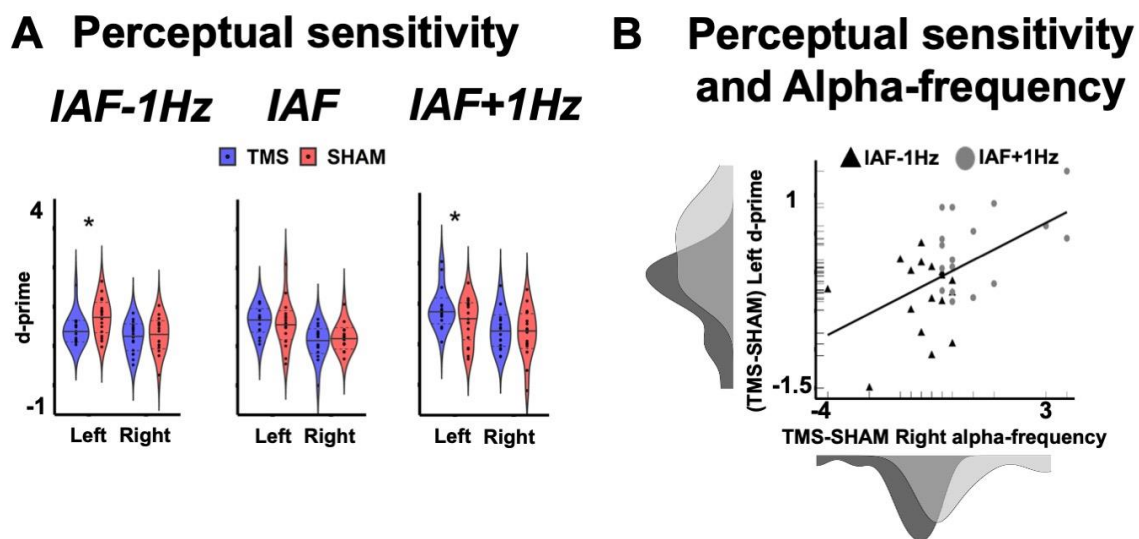
280

281 When examining the impact of entrainment on behavior (Figure 4A), we found
282 that speeding up or slowing down alpha oscillations had a direct impact on
283 performance (STIMULATION \times GROUP \times HEMIFIELD interaction ($F(1,48)=3.25$,
284 $p=.047$, $\eta p^2=.119$). Specifically, slowing-down pre-stimulus alpha-frequency led to
285 lower d' scores in the active rhythmic-TMS condition (relative to sham stimulation)
286 exclusively in the hemifield contralateral to stimulation ($t(16)=2.67$, $p=.017$, $d=.65$). In
287 contrast, speeding-up pre-stimulus alpha-frequency led to higher d' values during
288 active rhythmic-TMS (relative to sham stimulation), exclusively in the contralateral
289 hemifield ($t(16)=2.52$, $p=.023$, $d=.61$). Finally, entrainment at individual alpha-
290 frequencies did not yield differences in task accuracy, as predicted (all $t_s(16) < 1.19$,
291 all $p_s > .252$, all $d_s < .29$). We further tested whether the impact of rhythmic-TMS on
292 EEG oscillatory activity could account for the magnitude of the behavioral modulation
293 induced by the TMS protocol (Figure 4B). To do so, we examined the relationship
294 between sham-corrected performance and sham-corrected entrained frequency
295 across participants (IAF ± 1 Hz groups included). The results reveal that a significant
296 positive relationship exists between the TMS-induced change in oscillatory peak

297 frequency and performance gain ($R^2=0.29$, $p=.001$), further confirming a link
 298 between alpha-frequency and performance accuracy.

299 Our results thus far indicate that pre-stimulus alpha-frequency, but not alpha-
 300 amplitude, has a causative role in sampling sensory input, accounting for visual
 301 accuracy.

302



303

304 **Figure 4. Results Experiment 2: rhythmic-TMS entrainment causally links**
 305 **alpha speed to perceptual accuracy.** A. Perceptual sensitivity. Results are
 306 presented for three groups of participants (IAF \pm 1Hz and IAF stimulation protocol).
 307 Perceptual sensitivity is quantified in d' scores. Violin plots of d' are reported for
 308 rhythmic-TMS (TMS) and SHAM-control stimulation, and separately for the left and
 309 right hemifields. Data are presented as median (full line) \pm 1 quartile (dashed line). B.
 310 Perceptual sensitivity and alpha-frequency. Relationship between TMS-induced
 311 differences in alpha-frequency in the stimulated (right) hemisphere (computed as a
 312 difference in alpha-frequency between TMS and SHAM stimulation) and differences
 313 in accuracy in the opposite (left) hemifield (computed as a difference in d' score
 314 between TMS and SHAM stimulation), across the slower (IAF-1Hz group,
 315 represented as black triangles) and faster rhythmic-TMS groups (IAF+1Hz group,
 316 represented as grey circles). Density distributions of the two variables across the two
 317 groups are also presented along the corresponding axes. t-test statistical
 318 significance is reported ($*p<.05$).

319

320 **Alpha-amplitude dynamics shape subjective confidence and metacognition,**

321 **not accuracy**

322 Another goal of Experiment 2 was to determine whether alpha-amplitude
323 dynamics causally shape subjective representation and interpretation of perceptual
324 performance. However, confidence levels and metacognitive abilities – as measured
325 via confidence mean and meta-d' scores²⁹ respectively – appeared not to be
326 affected across the three different stimulation protocols nor between the two
327 hemifields, as neither the main effects of GROUP, HEMIFIELD and STIMULATION,
328 nor their interactions, reached significance (all $F_s(2,48) < 2.72$, all $p_s > .076$, all
329 $\eta p^2 < .102$). The short-term nature of entrainment effects might explain these null
330 results, as they are limited to a few hundreds of milliseconds following
331 stimulation^{37,39,40}. This is long enough for pre-stimulus TMS entrainment to influence
332 the primary accuracy response, as this was collected immediately after stimulus
333 presentation. The secondary, higher decision confidence response, however, which
334 was associated with pre-stimulus EEG alpha-amplitude, was collected only 1.5-2 sec
335 post-stimulus (through the confidence prompt) and hence occurred >1 sec after
336 rhythmic-TMS offset (see Figure 1B), when entrainment effects might not be
337 sufficiently sustained anymore^{37,41}. Therefore, in order to further assess the causal
338 role of alpha-amplitude dynamics in perceptual awareness, and particularly in
339 metacognitive abilities, we ran a third follow-up experiment aimed at entraining post-
340 stimulus alpha-amplitude in seventeen participants (12 women; mean age=22.47,
341 SE=0.66). This group received 5-pulse rhythmic-TMS trains that were tailored to
342 their individual alpha-frequency with pulses applied just before the confidence
343 prompt, i.e. after stimulus presentation (see Figure 1C). The aim of this protocol was
344 to enhance alpha-amplitude by rhythmic-TMS without affecting alpha-speed.
345 Importantly, analysis of the alpha-amplitude in the post-stimulus period in
346 Experiment 1 justified the timing of this stimulation, as alpha-amplitude after stimulus

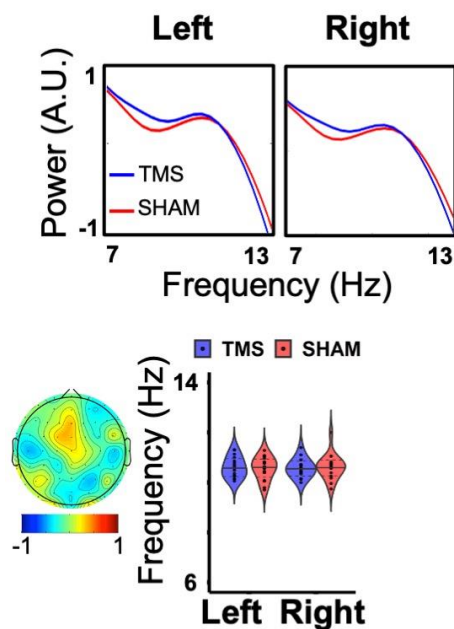
347 presentation (i.e. the time window of stimulation in Experiment 3) was related to
348 subjective confidence (with lower contralateral alpha-amplitude leading to high
349 confidence responses) and metacognitive abilities.

350 EEG analyses in Experiment 3 revealed a maximal entrainment effect in
351 broadband alpha-amplitude prior to the confidence prompt during active rhythmic-
352 TMS relative to sham stimulation at the stimulated site
353 (HEMISPHERE \times STIMULATION interaction: $F(1,16)=6.91$, $p=.002$, $\eta p^2=.302$).
354 Moreover, as expected, the rhythmic-TMS trains at IAF did not have any effect on
355 the alpha frequency measured prior to confidence judgment (all $F_s(1,16)< 0.19$, all
356 $p_s>.666$, all $\eta p^2<.012$) (Figure 5A, B). Crucially, this selective modulation of alpha-
357 amplitude right before confidence judgment allowed us to causally test the impact of
358 alpha-amplitude on metacognitive abilities vs. subjective confidence ratings. Our
359 results show clear effects on metacognition, as highlighted by distinct modulations of
360 meta- d' scores, between active rhythmic-TMS and sham stimulation, depending on
361 hemifield (HEMIFIELD \times STIMULATION interaction: $F(1,16)=4.73$, $p=.045$, $\eta p^2=.228$)
362 (Figure 5C). Specifically, higher alpha-amplitudes prior to the confidence prompt led
363 to lower meta- d' scores during active rhythmic-TMS vs. sham stimulation, exclusively
364 in the contralateral hemifield ($t(16)=2.74$, $p=.014$, $d=.66$). Importantly, these induced
365 changes in post-stimulus alpha-amplitude had a selective impact on metacognitive
366 abilities and not on confidence measures or on perceptual accuracy (all
367 $F_s(1,16)<.82$, all $p_s>.379$, all $\eta p^2<.049$), thus confirming the role of post-stimulus
368 alpha-amplitude in higher-level post-perceptual decision making.

369 Finally, we tested whether individual differences in TMS-induced post-stimulus
370 alpha-amplitude modulations could account for the level of metacognitive abilities. To
371 do so, we analyzed the relationship between sham-controlled TMS-induced alpha-

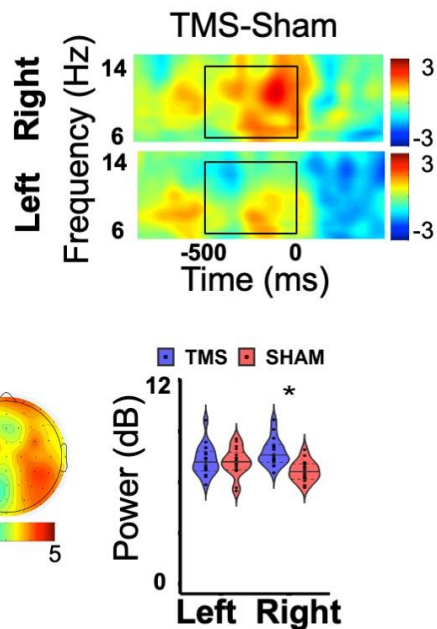
372 amplitude and sham-controlled meta-d' levels for stimuli presented in the
 373 contralateral hemifield. We found a significant inverse relationship, confirming that
 374 the higher the impact of rhythmic-TMS on alpha-amplitude, the lower the resulting
 375 level of metacognition of the individual response ($R^2=0.27$, $p=.032$; Figure 5D).
 376 These results strongly support a role of post-stimulus alpha-amplitude in selectively
 377 shaping our metacognitive abilities, with higher post-stimulus alpha-amplitude
 378 leading to lower metacognition.

A Alpha Frequency



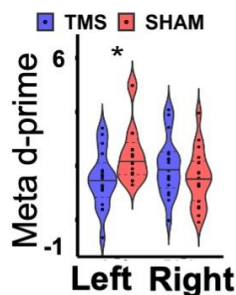
B

Post-stimulus Alpha Amplitude



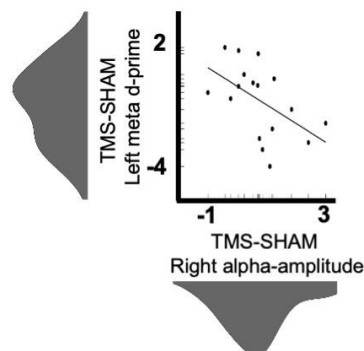
C

Metacognitive Abilities



D

Metacognitive Abilities and Post-stimulus Alpha-amplitude



379

380 **Figure 5. Results Experiment 3: rhythmic-TMS entrainment causally links**
381 **post-stimulus alpha-amplitude to metacognitive abilities.** A. (Upper) Averaged
382 Alpha-frequency is represented as the z-scored mean power ($10 \cdot \log_{10}[\mu\text{V}^2/\text{Hz}]$)
383 spectrum in a pre-confidence time period (850 1500) in the right (stimulated)
384 hemisphere (electrode cluster: O2,PO4,PO8) and in the left (non-stimulated)
385 hemisphere (electrode cluster: O1,PO3,PO7) for rhythmic-TMS and SHAM-control
386 stimulation. (Lower) Violin plots report peak frequency during TMS and SHAM,
387 separately for the left and right (stimulated) hemisphere. Data are presented as
388 median (full line) ± 1 quartile (dashed line); Topography represents the difference in
389 alpha-frequency between TMS and SHAM stimulation. B. (Upper) Post-stimulus
390 alpha-amplitude reported as a time-frequency plot of the difference between TMS
391 and SHAM stimulation in the right (stimulated) hemisphere (electrode cluster:
392 O2,PO4,PO8) and in the left (non-stimulated) hemisphere (electrode cluster:
393 O1,PO3,PO7). Black boxes denote regions of statistical analyses (alpha-band 7-
394 13Hz in the pre-confidence stimulation period (1000,1500)). (Lower) Violin plots
395 report alpha-power during TMS and SHAM stimulation, and separately for the left
396 and right (stimulated) hemisphere. Data are presented as median (full line) ± 1
397 quartile (dashed line). Topography represents the difference in alpha-amplitude
398 between TMS and SHAM stimulation. C. Metacognitive Abilities, quantified via meta-
399 d' scores. Violin plots of meta d' for TMS and SHAM-control stimulation, and
400 reported separately for the left and right hemifields. Data are presented as median
401 (full line) ± 1 quartile (dashed line). D. Metacognitive Abilities and Post-stimulus
402 Alpha-amplitude. Relationship between rhythmic-TMS-evoked differences in alpha-
403 amplitude in the stimulated (right) hemisphere (computed as a difference in alpha-
404 amplitude between TMS and SHAM stimulation) and differences in metacognition in
405 the opposite (left) hemisphere (computed as a difference in meta- d' score between
406 TMS and SHAM stimulation). Density distributions of the two variables are also
407 presented along the corresponding axes. Two-tailed t-test statistical significance is
408 reported ($*p < .05$). A.U.=arbitrary units; μV =microvolt; Hz=Hertz; ms=milliseconds;
409 dB=decibel.
410

411 **Discussion**

412 The oscillatory underpinnings of conscious perception have been the focus of
413 many studies, yet they remain largely unknown. A number of studies have previously
414 reported that pre-stimulus alpha oscillations over occipital sites might play a role in
415 human perceptual performance prediction^{e.g.16,42–45}, highlighting the potential
416 existence of a direct link between levels of alpha activity, cortical excitability and
417 perceptual sensitivity. Recent findings^{17,18,20,33,46} have, however, challenged these
418 past interpretations, and have highlighted the need to dissociate the processes that
419 shape perceptual sensitivity from those that shape the subjective interpretation of a

420 sensory event²⁸. Here, we disentangle the oscillatory dynamics of these two
421 processes and go beyond a correlative approach. By using an information-based
422 rhythmic-TMS protocol³⁶, we demonstrate that distinct markers of alpha activity have
423 a causal role in shaping our conscious perception, a role that goes beyond that of a
424 simple epiphenomenon. By directly manipulating alpha-frequency and -amplitude at
425 the site of stimulation^{47,48}, we were able to dissociate perceptual sensitivity from the
426 subjective representation and interpretation of a sensory event, thus demonstrating
427 their dualistic nature.

428 Our findings show that the speed of occipital alpha activity has a crucial and
429 selective role in modulating perceptual sensitivity. This adds to previous reports
430 showing that alpha cycles account for sampling sensory information into discrete
431 units/perceptual frames (initially proposed by⁴⁹ and reviewed in¹²). From this, one
432 might expect that higher frequency would translate in higher accuracy when
433 information can be sampled over many cycles. But why would this effect show even
434 when a sensibly short-lasting stimulus, certainly shorter than one alpha cycle, is
435 presented, as in our case? With our experimental design (60ms stimulus duration),
436 there is only one chance (sample) to capture the stimulus within an alpha cycle. And
437 what would this tell us about the underlying mechanism? To address this, we provide
438 here an exemplar account of the impact of frequency variations on sampling efficacy
439 for a 9Hz and 11Hz alpha oscillation. For these oscillations, cycles will range
440 between 110ms (for 9Hz IAF) and 90ms (for 11Hz IAF). However, processing
441 abilities will vary within the cycle, with a rapid fluctuation from a high to low
442 excitability phase (from alpha peak to trough)⁵⁰⁻⁵³. Hence, sampling is expected to
443 occur in one half of this cycle only, i.e. during ~55ms for 9Hz and ~45ms for 11Hz,
444 respectively. Our data suggest that this sampling is more effective with higher than

445 lower alpha frequencies, even with stimuli as short as 60ms, suggesting that
446 evidence accumulation already starts to differ within one sampling sweep across
447 variations of alpha-frequencies. This can be explained by enhanced processing
448 capacities for shorter than longer cycles, because with the shorter sampling phases
449 (~45ms), our short-lasting stimulus (60ms) is more likely to be fully comprehended in
450 one perceptual frame. For stimuli of longer durations (e.g. 1000ms), one would
451 expect repeated sampling sweeps to further add to this difference, as more full-
452 sample sweeps can be packed in 1sec at high than low frequencies (11 vs. 9
453 sweeps, for 11Hz vs 9Hz). In sum, here we claim that in line with existing
454 literature^{23,24,33} higher frequencies are expected to aid temporal resolution by
455 creating more sampling frames per second; but our data show that, at the same
456 time, in the context of our specific experiment, higher frequency also means that less
457 time is employed to create a single sampling frame, leading to higher processing
458 capacities.

459 Our EEG findings furthermore show an inverse relationship between levels of
460 alpha-amplitude and subjective confidence confirming previous findings¹⁷⁻¹⁹. Indeed,
461 pre-stimulus alpha-amplitude has been proposed to relate to internal decision-
462 making variables^{18,20}, rather than perceptual accuracy per se. Yet, our experimental
463 manipulation by rhythmic-TMS could not verify the existence of a causal link
464 between pre-stimulus alpha-amplitude and confidence. However, several studies
465 have concluded that our sense of confidence is also determined by processes that
466 occur after we make a choice, thus integrating sensory evidence and improving our
467 “metacognitive accuracy”, namely the extent to which our confidence is consistent
468 with our probability of being correct^{e.g.31,54,55}. Examining post-stimulus alpha-
469 amplitude, Experiments 1 and 3 demonstrate that after lateralized stimuli are

470 presented, perceptually relevant, post-stimulus alpha-amplitude become focused in
471 the hemisphere contralateral to stimulus presentation, with lower alpha-amplitude
472 leading to higher perceptual confidence. Moreover, these levels of post-stimulus
473 alpha desynchronization directly account for metacognitive abilities across
474 participants and can be causally manipulated by rhythmic-TMS. These latter results
475 suggest that post-stimulus alpha modulations may reflect the integration of
476 confidence judgment with the accumulated evidence after stimulus presentation to
477 update and adjust metacognitive decisions^{31,55,56}. Taken together, these results
478 speak in favor of a relevant role of alpha-amplitude in post-perceptual decision
479 making. Therefore, it might be possible that pre-stimulus alpha-amplitude dictates
480 the initial level of perceptual bias (effects observed for confidence bilaterally, but not
481 metacognitive effects), that subsequently integrates sensory evidence brought by the
482 stimulus itself (reflected in hemisphere-specific processes), resulting in post-
483 perceptual estimation of the performance.

484 While our experiments show that alpha-frequency and –amplitude, and hence
485 sensitivity and confidence, are dissociable entities, these processes likely work in
486 concert in more ecological situations to maximize the efficiency of our conscious
487 experience. We observed that the entrainment effects on oscillation and perception
488 showed corresponding topographic/retinotopic distributions, with perception being
489 exclusively modulated in the hemifield contralateral to the stimulated site, suggesting
490 that the oscillatory substrates of effective sampling and subjective confidence could
491 be oriented in space to optimize the allocation of attention resources. Therefore,
492 under controlled conditions (for example by presenting informative cues⁵⁷ or in
493 predictive contexts⁵² that are associated with spatial priors), one might expect the
494 spatially specific co-occurrence of alpha-frequency and -amplitude modulation that is

495 contralateral to the to-be-attended or expected location^{59,60}. Future research into the
496 inter-dependency of these two circuits may shed new light on different
497 neuropsychological phenomena. For example, the failure to integrate perceptual
498 processes and their subjective interpretation might lead to altered cognitive
499 experiences, such as confabulations or the formation of false representations and
500 memories, with relevant implications for clinical and forensic neuropsychology. The
501 failure to integrate perceptual processes and their subjective interpretation may also
502 lead to conscious departure from sensory events in acute schizophrenia patients⁶¹.

503 In conclusion, our results point to a functional dissociation between the
504 accuracy of what we see and our interpretation of it. We reveal that the sampling of
505 visual information and its subjective interpretation, which are strongly inter-
506 dependent in everyday life, are dissociable in terms of neural mechanisms in
507 oscillatory activity. Specifically, alpha-frequency and -amplitude reflect the activity of
508 these two independent mechanisms that serve complementary functions. Alpha-
509 frequency represents a spatial and temporal sampling mechanism^{27,62-64} that shapes
510 perceptual sensitivity. By contrast, alpha-amplitude dictates more liberal vs
511 conservative choices in confidence judgments, further modulated with incoming
512 sensory evidence, thus having post-perceptual effect on how these subjective
513 confidence judgments can distinguish between correct and incorrect decisions^{17,19}.
514 How these mechanisms interact to give rise to an integrated (or not) sense of our
515 perceptual environment, is yet to be addressed. However, we demonstrate that
516 these oscillatory processes can be selectively modulated by non-invasive
517 neurostimulation, offering a foundation to future translational neuroscience
518 approaches and clinical applications.

519

520 **Acknowledgments**

521 FDG is supported by the Ministero della Salute (SG-2018-12367527); AA is
522 supported by Fondazione del Monte di Bologna e Ravenna (339bis/2017), Bial
523 Foundation (347/18) and Ministero dell'Istruzione, dell'Università e della Ricerca
524 (2017N7WCLP); VR is supported by the Bial Foundation (204/18);

525

526 **Author contributions**

527 VR conceived the project; VR, FDG, JT, CR, AA, GT designed the experiment;
528 VR, FDG, EM, PDL, JT, CR, Implemented the experiment; JT, EM, PDL and CR
529 conducted the experiment; FDG and JT analysed data; FDG, JT and VR wrote the
530 first draft of the paper. VR, FDG, EM, PDL, JT, CR, AA GT contributed to the final
531 draft of the paper.

532

533 **Declaration of Interests**

534 The authors declare no competing interests.

535

536

537

538

539

540

541

542

543

544

545

546 **STAR Methods**

547 **Resource availability**

548 *Lead contact.* Further information and requests for resources and reagents should
549 be directed to and will be fulfilled by the Lead Contact, Vincenzo Romei
550 (vincenzo.romei@unibo.it).

551

552 *Materials availability.* See the Key resources table for information about resources.
553 This study did not generate new unique reagents.

554

555 *Data and code availability.* The datasets generated during this study have been
556 made publicly available through the Open Science Framework (<https://osf.io/e4bnj/>).
557 Any additional information required to reanalyse the data reported in this paper is
558 available from the lead contact upon request.

559

560 **Experimental model and subject details**

561 ***Experiment 1***

562 *Participants:* Twenty-four healthy volunteers (12 women, 12 men; mean age=
563 23.2, SE=2.61) with normal or corrected vision participated in Experiment 1. Sample
564 size was determined based on previous literature. Specifically, previous EEG studies
565 on the role of pre-stimulus alpha in conscious perception considered a sample size
566 between 10 and 26 participants^{18,33,65,66}. In addition, post-hoc power analysis (G-
567 power 3.1) revealed that, for all significant ANOVA effects in our study, values of
568 Power (1- β err prob) are >0.95. All participants were recruited at the Centre for
569 Studies and Research in Cognitive Neuroscience in Cesena, Italy. The study was

570 conducted in accordance with the Declaration of Helsinki. All participants gave
571 written informed consent to participate in the study, which was approved by the
572 bioethics committee of the University of Bologna.

573 ***Experiment 2***

574 *Participants.* Fifty-one healthy volunteers (25 females, 26 males; mean age \pm
575 SE = 23.39 \pm 0.36 years) took part in Experiment 2. Sample size was determined
576 based on previous literature. Specifically, previous TMS studies on oscillatory
577 entrainment considered a sample size between 7 and 17^{35,37,67–71}. In addition, post-
578 hoc power analysis (G-power 3.1) revealed that, for all significant ANOVA effects in
579 our study, values of Power (1- β err prob) are >0.95. All of the participants had
580 normal or corrected-to-normal vision and met TMS safety criteria by self-report. All
581 participants gave written informed consent before taking part in the study, which was
582 conducted in accordance with the Declaration of Helsinki and approved by the local
583 ethics committee. Here, subjects were randomly assigned to one of three groups,
584 with distinct stimulation protocols (see Methods details section): IAF-1Hz (group
585 1=mean age 22.64 \pm 0.52, nine females), IAF (group 2=mean age 23.88 \pm 0.52, eight
586 females) and IAF+1Hz (group 3=mean age 23.88 \pm 0.77, eight females), each
587 containing 17 participants.

588 ***Experiment 3***

589 *Participants.* Seventeen healthy new volunteers (12 women, 5 men; mean
590 age=22.47, SE=0.66) were recruited for Experiment 3.

591

592 **Method details**

593 ***Experiment 1***

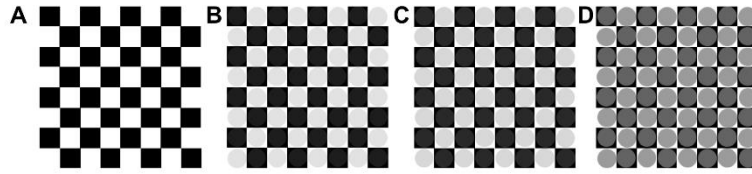
594 *Stimuli and task procedure.* Participants were comfortably seated in front of a
595 CRT monitor (100Hz refresh rate) at a viewing distance of 57cm. A PC running E-
596 Prime software (Psychology Software Tools, Inc., USA) controlled stimulus
597 presentation and responses registration. During the main experimental procedure
598 (main task), each trial consisted of a *primary visual detection task*, in which
599 participants responded to visual stimuli displayed on the computer screen, and a
600 *secondary confidence task*, in which participants rated the level of confidence in their
601 perception on a scale of 1 to 4, where 1=no confidence at all; 2=little confidence;
602 3=moderate confidence; and 4=high confidence. At the beginning of each trial, a
603 white fixation cross was displayed on a grey background. The fixation cross was
604 presented in the centre of the screen for 2000ms and subtended a visual angle of
605 0.8°. Afterwards, an X (visual angle 2°) was created by rotating the fixation cross by
606 45 degrees. The cue appeared for a variable time period (time jitter between 2000
607 and 3000ms), immediately followed by the primary task stimulus. The stimulus could
608 appear with equal probability on the right or left visual field. These stimuli were
609 presented at 4.1°/3.7° eccentricity (horizontal/vertical) in the lower part of the left
610 visual field (LVF) or right visual field (RVF) for 60ms. The primary task stimulus could
611 be either a catch stimulus (50% of trials) or a target stimulus (50% of trials). Catch
612 stimuli consisted of 8x8 black and white checkerboards (height=4cm; width=4cm.
613 visual angle=15.9°). Target stimuli consisted of the same checkerboard containing
614 iso-luminant grey circles, which contrasted the black and white parts of the
615 checkerboard. Participants were prompted to press the spacebar on the keyboard
616 with their right index finger whenever they detected the circles embedded in the
617 checkerboard. Primary response speed was not stressed over perceptual accuracy,
618 but a time limit of 2000ms was given. After this primary response, confidence ratings

619 were collected. The Italian version of the question: “How confident are you about
620 your percept?” was presented until participants rated their confidence. Confidence
621 was rated on a 4-points Likert scale, from “no confidence at all” to “high confidence”,
622 and was reported by pressing the corresponding number on the keyboard with the
623 left index finger. Notably, here the confidence rating reflects a participant’s level of
624 subjective certainty in having correctly perceived the stimulus⁷². After rating their
625 confidence, a new trial started with the presentation of a new fixation cross. The
626 main task consisted of 5 blocks with 60 trials per block (total trial number=300) and
627 lasted on average 90min.

628

629 *Titration session.* A titration session was run before the main experimental
630 session in order to set stimuli contrast ratios corresponding to each individual’s 50%
631 perceptual threshold. Iso-luminant circles of 8 different contrast ratios (RGB
632 contrasts on black/white background: 28/227, 32/223, 36/219, 40/215, 44/211,
633 48/207 and 100/155) were presented together with catch trials (checkerboards
634 without iso-luminant circles). Please note examples of stimuli of different contrasts:
635 A. Catch Stimulus B. Low Contrast Stimulus (RGB contrasts: 30/225) C. High
636 Contrast Stimulus (RGB contrasts:40/215) D. Maximum Contrast Stimulus (RGB
637 contrasts:100/155).

638 To account for individual biases among participants in their response to catch
639 trials, a false alarm rate was considered, together with target stimuli of different
640 contrast for the calculation of the sigmoid function. For each iso-luminant contrast,
641 individual performance was then entered to calculate the sigmoid function.



642

643 **Figure 6. Examples of stimuli of different contrasts. A. Catch Stimulus B.**
 644 **Low Contrast Stimulus (RGB contrasts: 30/225) C. High Contrast Stimulus (RGB**
 645 **contrasts:40/215) D. Maximum Contrast Stimulus (RGB contrasts:100/155)**
 646

647 Data were analyzed using the following formula to calculate the threshold value
 648 (y):

649

$$650 \quad y = \frac{100}{1 + e^{-\frac{x-c}{d}}}$$

651

652 Where x is the contrast value, c is the inflection point of the curve and d is the
 653 slope of the sigmoid.

654 The corresponding inflection point was selected as the bias-adjusted threshold,
 655 which was used for stimulus presentation during the experiment. In Experiment 1,
 656 detection performance threshold during the main task (M=56.9%, SE=3.69%) was
 657 not statistically different from the bias-adjusted threshold (M=51.58%, SE=0.48%)
 658 calculated during the titration session, ($t(24)=1.68$, $p=.11$, $d=0.34$). Across
 659 participants, the selected luminance contrast ratios during the main task ranged
 660 between 20/235 and 50/205 RGB points (M=32/223, SE=12).

661

662 **Experiment 2**

663 Both Experiment 2 and Experiment 3 implemented a rhythmic-TMS
664 entrainment protocol with concurrent EEG recording. The timing of rhythmic-TMS
665 pulses differed between the two experiments.

666 *Stimuli and task procedure.* Stimuli and tasks in Experiment 2 were the same
667 as those described for Experiment 1, with the main difference being the active
668 manipulation of alpha activity via an entrainment protocol.

669 Entrainment of the intrinsic oscillatory alpha activity was achieved using
670 rhythmic transcranial magnetic stimulation (rhythmic-TMS). Specifically, pre-stimulus
671 alpha activity was fine-tuned relative to individual alpha-frequency using rhythmic
672 five-pulse TMS bursts in which the time lag between pulses was manipulated
673 depending on the group^{21,73}. In order to induce changes in the alpha-frequency cycle
674 length, rhythmic-TMS was applied at a slower or faster pace, relative to a
675 participant's individual alpha-frequency. To selectively modulate alpha-amplitude, the
676 frequency of the rhythmic-TMS pulse trains was matched to the intrinsic individual
677 alpha-frequency of the participant, thus enhancing the synchronization of neural
678 firing and phase alignment without influencing the speed of alpha activity. In this
679 way, rhythmic-TMS pulse trains could occur at three different frequencies: at the
680 individual alpha-frequency of the participant to manipulate pre-stimulus alpha-
681 amplitude (IAF group); at 1Hz lower than the individual alpha-frequency (IAF-1Hz
682 group) to slow-down pre-stimulus alpha-frequency; or at 1Hz higher than the
683 individual alpha-frequency (IAF+1Hz group) to speed-up pre-stimulus alpha-
684 frequency. In all groups, the last TMS-pulse coincided with the stimulus appearance.

685 Biphasic stimulation was applied using a Magstim Rapid Transcranial Magnetic
686 Stimulator via a 70mm figure-of-eight coil (Magstim Company, UK) of maximum field
687 strength ~1.55T. As systematic differences in visual cortex excitability do not seem

688 to be present between the hemispheres^{34,74–76}, TMS bursts were delivered only to
689 the right occipital site (at O2 electrode position), with the coil surface tangent to the
690 scalp, and the handle oriented perpendicular to the medial plane of the subjects
691 head (latero-medial current direction). Moreover, pulse intensity was kept fixed at
692 60% of the maximum stimulator output (MSO)^{34,77–79}, roughly corresponding to
693 previously reported phosphene thresholds^{80–84}. No subject reported to have
694 perceived phosphenes during the execution of the task. Within-subject sham control
695 stimulation was implemented in order to account for any non-specific rhythmic-TMS
696 effects. To do so, a modified coil was used that provided enough distance from the
697 scalp to ensure the absence of stimulation, while at the same time maintaining coil
698 position, as well as tactile and acoustic sensations. Each participant underwent three
699 consecutives rhythmic-TMS and sham blocks (resulting in a total of 900 active
700 rhythmic-TMS pulses), whereas rhythmic-TMS/sham stimulation block order was
701 randomized. Therefore, the experimental session consisted of 6 blocks with 60 trials
702 per block (total trial number=360) (see also Experiment 1), with short breaks
703 between the blocks (overall average task duration of 50 minutes). The rhythmic-TMS
704 design was in line with current safety guidelines⁸⁵.

705

706 *Titration session.* Titration was run as for Experiment 1. Additionally, in the
707 second experiment, during the titration session, individual alpha peak frequency
708 (defined as the maximum local power in the alpha-frequency range) was determined.
709 A total of six minutes resting-state EEG (three minutes with eye closed and three
710 minutes with eyes open, and with gaze on a fixation cross on the screen) was
711 recorded from 8 Ag/AgCl parieto-occipital electrodes (O1,P3,PO3,PO7; O2,P4,PO4,
712 PO8). Individual alpha-frequency peak was calculated from the power spectra of the

713 eyes open condition, applying a Fast Fourier Transformation. In line with Experiment
714 1 (showing a local alpha power maxima over O2) and previous studies, alpha-
715 frequency was calculated from the O2 electrode^{21,83}, over which rhythmic-TMS was
716 subsequently applied (see above). The identified individual alpha-frequency was
717 used to calibrate rhythmic-TMS frequency.

718

719 ***Experiment 3***

720 *Stimuli and task procedure.* The stimuli and task for Experiment 3 were the
721 same as those used for Experiment 2, the main difference being the timing of the
722 manipulation of alpha activity via an entrainment protocol.

723 Specifically, Experiment 3 aimed to selectively enhance post-stimulus alpha-
724 amplitude, prior to the confidence prompt. As such, only one entrainment protocol
725 was applied (i.e. stimulation at the individual alpha-frequency). While in Experiment
726 2, the final pulse of the rhythmic-TMS-train coincided with stimulus onset, in
727 Experiment 3, the final rhythmic-TMS pulse coincided with the onset of the
728 confidence prompt.

729 Stimulation site, coil orientation, stimulation intensity, control conditions and
730 number of pulses were the same as those used in Experiment 2.

731

732 *Titration session.* The titration session was conducted as in Experiment 2.

733

734 **Quantification and Statistical Analysis**

735 ***Experiment 1***

736 *Psychophysiological recording – paradigm and acquisition.* EEG data were
737 collected during the main task in Experiment 1 from 64 Ag/AgCl electrodes

738 (Fp1,Fp2,AF3,AF4,AF7,AF8,F1,F2,F3,F4,F7,F8,FC1,FC2,FC3,FC4,FC5,FC6,FT7,F
739 T8,C1,C2,C3,C4,C5,C6,T7,T8,CP1,CP2,CP3,CP4,CP5,CP6,TP7,TP8,P1,P2,P3,P4,
740 P5,P6,P7,P8,PO3,PO4,PO7,PO8,O1,O2,Fpz,AFz,Fz,FCz,Cz,CPz,Pz,POz,Oz) and
741 from the right mastoid with Brain Vision recorder software (Brain Products, Munich,
742 Germany). The left mastoid was used as reference, and the ground electrode was
743 placed on the right cheek. The electrooculogram (EOG) was recorded from above
744 and below the left eye and from the outer canthi of both eyes. EEG and EOG were
745 recorded with a band-pass filter of 0.01–100Hz, at a sampling rate of 1000Hz, which
746 was re-sampled to 500Hz offline. The impedance of all electrodes was kept below
747 10k Ω . EEG data were pre-analyzed using custom made routines in MatLab R2013b
748 (The Mathworks, Natick, MA, USA). EEG data were re-referenced off-line to the
749 average of all electrodes and filtered with a 0.5–30Hz pass-band. Epochs were
750 extracted stimulus-locked from -1500ms to 2500ms. Artefact-contaminated epochs
751 were excluded using the pop_autorej function in EEGLAB v13.0.1⁸⁶, which first
752 excludes trials with voltage fluctuations larger than 1000 μ V, and then excludes trials
753 with data values outside five standard deviations (mean=9.7% SE=2.9% of trials
754 removed). Subsequently, EOG artefacts were corrected by a procedure based on a
755 linear regression method (lms_regression function in MatLab R2013b)⁸⁷. Because
756 perceptually relevant, pre-stimulus alpha activity shows hemispheric lateralization,
757 relative to upcoming stimulus location, we recoded electrode positions as
758 contralateral versus ipsilateral to the hemifield of stimulus presentation (resulting in
759 all contralateral activity being on one side, which was conventionally defined to be
760 the right), i.e. for RVF-stimulus epochs, data from the contralateral (left) electrodes
761 were copied and flipped to right-sided electrodes, electrodes on the midline were not
762 flipped or recoded.

763 In order to identify the individual alpha-frequency peak during the task, data
764 epochs in the cue-stimulus period (i.e. pre-stimulus alpha from -1000ms to stimulus
765 presentations, baseline between -1500 and -1000ms) were analyzed with a fast
766 Fourier transformation (MatLab function spectopo, frequency resolution: 0.166Hz).
767 Power was calculated separately for each subject and condition and was normalized
768 by z-score decibel ($\text{dB}=10*\log_{10}[-\text{power}/\text{baseline}]$) transformation at each frequency.
769 Individual alpha-frequency was defined as the local maximum power within the
770 frequency range 7-13Hz (i.e. alpha peak). Each subject showed a clear peak within
771 this alpha range. However, a peak in the alpha-band was not present at all
772 electrodes. For this reason, power spectra on all parietal-occipital electrodes were
773 visually inspected. Then, the contralateral electrode was selected for analyses where
774 alpha oscillation showed a clear peak²³. Homologous electrodes were selected for
775 the analyses in the ipsilateral hemisphere. This procedure identified the following
776 subset of parieto-occipital electrodes that were used separately for each subject and
777 condition to identify alpha-frequency in the cue-stimulus period: contralateral
778 electrodes (P8,PO8,PO4,O2), and ipsilateral electrodes (P7,PO7,PO3,O1).
779 Importantly, most of the participants (n=15) showed maximum power over electrode
780 O2.

781 The amplitude of alpha oscillations was calculated by time-frequency analyses
782 of data epoched from 2000ms before to 2000ms after the stimulus onset. Long
783 epochs prevent edge artefacts from contaminating time frequency power in the time
784 windows of interest. Spectral EEG activity was assessed by time-frequency
785 decomposition using a complex sinusoidal wavelet convolution procedure (between
786 2 and 25 cycles per wavelet, linearly increasing across 50 linear-spaced frequencies
787 from 2.0Hz to 50.0Hz) with the newtimef function from EEGLAB v13.0.1⁸⁶ and

788 custom routines in MatLab. The resulting power was normalized by decibel
789 ($\text{dB}=10*\log_{10}[-\text{power}/\text{baseline}]$) transformation at each frequency, using a single trial
790 baseline between -1000 and -500 preceding stimulus onset. This long baseline
791 window was used to increase the signal-to-noise ratio during the baseline period and
792 is frequently applied in time frequency analyses^{88,89}. This procedure was applied
793 separately for each subject and condition. Mean alpha (7-13Hz) amplitude was
794 computed separately for each condition in the cue-stimulus interval (-500 to 0ms)¹⁸
795 and in the post-stimulus interval (0 to 900ms), which corresponds to the pre-
796 confidence prompt time period. In order to identify electrode clusters for the analyses
797 of alpha-amplitude, we used the same procedure as for alpha-frequency. For alpha-
798 amplitude, the following subsets of posterior contralateral (P2,P4,P8,PO4,PO8,O2)
799 and ipsilateral (P1,P3,P7,PO3,PO7,O1) electrodes were used for the analyses.
800 Importantly, as for alpha-frequency, most of the participants (n=18) showed
801 maximum alpha-amplitude over electrode O2.

802

803 *Statistical Analyses.* First, trials were sorted according to objective accuracy
804 (i.e. into correct and error trials). Correct trials consisted of correctly detected target
805 trials (i.e. hits, where participants pressed the spacebar after a target trial) and
806 correctly detected catch trials (i.e. correct rejections, where participants did not press
807 the spacebar after a catch trial). Accordingly, error trials consisted of misses after
808 target trials and false alarms after catch trials. Then we compared participants with
809 high vs low perceptual sensitivity. Perceptual sensitivity was estimated using the d'
810 measure. In signal detection theory (SDT²⁸), d' reflects standardized measure of
811 discrimination abilities between the signal and the noise (type I sensitivity). d' was
812 calculated as $d'=z(H) - z(\text{FA})$, where z represents the z-scores of Hit rate (i.e. H, the

813 probability of correct reactions on target trials) and false alarms (i.e. FA, the
814 probability of incorrect reactions on catch trials²⁸).

815 Next, we focused on subjective confidence levels during correct trials (i.e. hits
816 and correct rejections). In order to compare confident vs. non-confident responses,
817 we aggregated high confident responses and low confident responses. In this way,
818 correct trials were divided in high confident (i.e. with a confidence rating of 3 or 4) and
819 low confident (i.e. with a confidence rating of 1 or 2) trials. Then, we compared
820 participants showing high vs low confidence or metacognitive performance. For
821 confidence analyses, the mean value of the confidence ratings was calculated for
822 each participant. Instead, metacognitive performance was quantified using the
823 computational method proposed by Maniscalco & Lau²⁹. This method quantifies the
824 efficacy of confidence ratings to discriminate between correct and erroneous
825 responses in a SDT model. The model accounts for the variance in task performance
826 to compute metacognitive sensitivity (type II sensitivity) on subjective confidence
827 rating. This method, previously described in detail and validated, can give a metric
828 (termed *meta-d'*) for metacognitive abilities^{29,90}. Briefly, the central idea is to link type
829 I and type II SDT models to compute the observed type II sensitivity. *meta-d'*
830 estimates the values, which maximize the fit between the observed type II data and
831 the parameter values of the *d'* type I SDT model. Here, *meta-d'* was calculated with
832 the function `fit_meta_d_SSE` in MatLab. This function minimizes the sum of squared
833 errors and estimates *meta-d'* using observed type II data and the empirical type I
834 criterion *c'*⁹⁰. In this way, *meta-d'* estimates, for instance, the relative likelihood to
835 report a high confidence rating after a correct response^{29,90}. Higher values of *meta-d'*
836 correspond to participants having better metacognitive abilities.

837 Within participants EEG analyses were performed separately for objective
838 accuracy and subjective confidence. For *Objective Accuracy*, we compared alpha
839 activity (both frequency and amplitude) in 2x2 repeated measures ANOVAs with the
840 factors ACCURACY (correct and incorrect) and HEMISPHERE (contralateral and
841 ipsilateral). For Subjective Confidence, analyses were performed on correct trials⁶⁵.
842 Alpha activity was analyzed for the factor CONFIDENCE (high and low confidence)
843 and for the factor HEMISPHERES (contralateral and ipsilateral) in 2x2 repeated
844 measures ANOVAs. Differences between conditions were tested by one or two-tailed
845 t-tests (planned comparisons).

846 Between participants EEG analyses were performed on perceptual sensitivity
847 and metacognitive performance. For perceptual sensitivity analyses, we divided
848 participants in two numerically equivalent groups using the median split of the d'
849 scores (high vs low d'). As for perceptual sensitivity, we also conducted between-
850 group analysis, by dividing participants in two numerically equivalent groups (high vs
851 low meta d' scores) on a median split basis of the meta-d' scores (i.e. metacognitive
852 performance). Differences between groups were tested by one or two-tailed
853 independent samples t-tests (planned comparisons).

854

855 *Pre-stimulus IAF and resting-state IAF.* As we have used resting IAF to target
856 pre-stimulus activity in experiments 2 and 3 (see results sections), we checked for
857 any potential difference between resting-state IAF and pre-stimulus IAF in
858 Experiment 1 to ensure adequacy of our approach, with the working hypothesis that
859 no significant differences should be observed. In this analysis, resting-state IAF was
860 defined as the maximum local power in the alpha-frequency range during the resting
861 state over a cluster of posterior electrodes (O1,P1,P3,P5,P7,Pz,POz,Oz,PO3,PO7;

862 O2,P2,P4,P6,P8,PO4,PO8), while pre-stimulus IAF was calculated in the same
863 electrode cluster across conditions in a time window between -1000ms and stimulus
864 presentation. The analysis was performed on 22 out of 24 participants as resting
865 EEG was not available for 2 participants. As expected, the two-tailed paired samples
866 t-test showed no differences ($t(21)=0.05$, $p=.968$, $d=.019$) between resting state IAF
867 ($M=10.81\text{Hz}$; $SE=0.21\text{Hz}$) and pre-stimulus IAF ($M=10.83\text{Hz}$; $SE=0.37\text{Hz}$).
868 Importantly, these results demonstrate that resting-state IAF and pre-stimulus IAF
869 are comparable within group.

870

871 ***Experiment 2***

872 *EEG recordings –acquisition and processing.* EEG data were collected for
873 Experiment 2 as for Experiment 1. However, in Experiment 2, a rhythmic-TMS pulse
874 train was applied during EEG recording. The resulting rhythmic-TMS artefacts were
875 identified and removed using an open-source EEGLab extension, the TMS-EEG
876 signal analyzer (TESA)⁹¹. First, EEG data were epoched around stimulus onset
877 (between -1500ms and 2500ms for Experiment 2 and between -1000ms and
878 2000ms for Experiment 3, due to differences in stimulation timing) and the linear
879 trend from the obtained epochs was removed. Then rhythmic-TMS pulse artefact
880 and peaks of rhythmic-TMS-evoked scalp muscle activities were removed (-10ms
881 +10ms) and cubic interpolation was performed prior to down-sampling the data (from
882 5000Hz to 1000Hz). Interpolated data was again removed prior to Individual
883 Component Analysis (ICA). Specifically, a fastICA algorithm was used
884 (pop_tesa_fastica function: <http://research.ics.aalto.fi/ica/fastica/code/dlcode.shtml>)
885 to identify individual components representing artefacts, along with automatic
886 component classification (pop_tesa_compselect function), where each component

887 was subsequently manually checked and reclassified when necessary. In this first
888 round of ICA, only components with large amplitude artefacts, such as rhythmic-
889 TMS-evoked scalp muscle artefacts, were eliminated. Data were again interpolated
890 prior to applying pass-band (between 1 and 100Hz) and stop-band (between 48 and
891 52Hz) Butterworth filters. Subsequently interpolated data were again removed prior
892 to the second round of ICA, in order to remove all other artefacts, such as blinks, eye
893 movement, persistent muscle activity and electrode noise. Then, rhythmic-TMS-
894 pulse period was interpolated and data was re-referenced to the average of all
895 electrodes. Finally, single trials were visually inspected and those containing residual
896 rhythmic-TMS artefact were removed. The described rhythmic-TMS artefact removal
897 procedure was applied to all EEG data, both for active rhythmic-TMS and sham
898 stimulations. On average, approximately one third of all epochs were removed
899 ($M=34.31\%$, $SE=1.72\%$) (remaining epochs mean=236.5 epochs, $SE=6.19$). A
900 graphical explanation of the artefact correction procedure is reported in the
901 supplemental information (see supplemental figure S3).

902 Alpha-frequency and alpha-amplitude were identified in a similar manner as per
903 Experiment 1. Alpha-frequency was defined as the local maximum power within the
904 frequency 7-13Hz range in a pre-stimulus period (-650ms to stimulus presentation).
905 Accordingly, pre-stimulus alpha-amplitude was calculated in the time frequency data
906 (as for Experiment 1). The time window of analyses corresponded to stimulation
907 period for both alpha-frequency and -amplitude. Near-stimulation parieto-occipital
908 electrodes in the right hemisphere (PO4,PO8,O2), along with analogous electrodes
909 in the left hemisphere (PO3,PO7,O1) were used for all of the analyses.

910

911 *Statistical analyses (behavioral data).* Behavioral data were analyzed
912 separately for perceptual sensitivity (d' score) and for confidence (mean of
913 confidence ratings) and metacognitive performance (meta d' score).

914

915 All scores were compared between the two HEMIFIELDS (left and right) and
916 two STIMULATION types (active rhythmic-TMS and sham) in three GROUPs of
917 participants (IAF \pm 1Hz, IAF), in 2x2x3 repeated measures mixed-model ANOVAs.

918

919 *Statistical analyses (EEG data).* Electrophysiological data were analyzed
920 separately for pre-stimulus alpha-amplitude and alpha-frequency. Therefore, both
921 parameters of alpha activity were compared between the two HEMISPHERES (left
922 and right parieto-occipital cluster) and the two STIMULATION types (active rhythmic-
923 TMS and sham) in three GROUPs of participants in 2x2x3 repeated measures
924 mixed-model ANOVAs. Differences between conditions were tested by two-tailed t-
925 test (planned comparisons).

926 Finally, the association between rhythmic-TMS-evoked differences in alpha-
927 frequency in the stimulated (right) hemisphere (computed as a difference in alpha-
928 frequency between active rhythmic-TMS and sham stimulation conditions) and
929 differences in perceptual sensitivity in the opposite (left) hemispace (computed as a
930 difference in d' score between active rhythmic-TMS and sham stimulation conditions)
931 was explored via linear regression.

932

933 ***Experiment 3***

934 *EEG recordings – acquisition and processing.* EEG data were recorded and
935 alpha-frequency and alpha-amplitude identified as in Experiments 1 and 2, with the

936 only difference being that the analysis window was moved to a time window
937 preceding the confidence prompt (850ms to 1500ms after stimulus presentation,
938 which corresponded to -650ms prior to the confidence prompt).

939

940 *Statistical analyses (behavioral data).* Behavioral data were analyzed
941 separately for perceptual sensitivity (d' score) and for confidence (mean of
942 confidence ratings) and metacognitive performance (meta d' score). All scores were
943 compared for the two HEMIFIELDS (left and right) and between different
944 STIMULATION types (active rhythmic-TMS and sham) in a 2x2 repeated measures
945 ANOVA.

946

947 *Statistical analyses (EEG data).* Electrophysiological data were analyzed
948 separately for alpha-amplitude and alpha-frequency. Moreover, differences in alpha-
949 amplitude and alpha-frequency were again compared between the two
950 HEMISPHERES (left and right) and between STIMULATION types (active rhythmic-
951 TMS and sham) in a 2x2 repeated measures ANOVA. Differences between
952 conditions were tested by two-tailed t-test (planned comparisons).

953 Finally, a linear regression model was used to determine whether rhythmic-
954 TMS-evoked differences in alpha-amplitude in the stimulated (right) hemisphere
955 (computed as a difference in alpha-amplitude between active rhythmic-TMS and
956 sham stimulation conditions) can predict differences in confidence levels in the
957 opposite (left) hemifield (computed as a difference in meta d' scores between active
958 rhythmic-TMS and sham stimulation conditions).

References

- 959 1. Hirst, W., Phelps, E.A., Meksin, R., Vaidya, C.J., Johnson, M.K., Mitchell, K.J.,
960 Buckner, R.L., Budson, A.E., Gabrieli, J.D.E., Lustig, C., et al. (2015). A ten-year follow-up
961 of a study of memory for the attack of September 11, 2001: Flashbulb memories and
962 memories for flashbulb events. *Journal of Experimental Psychology: General* *144*, 604–623.
- 963 2. Garry, M., Manning, C.G., Loftus, E.F., and Sherman, S.J. (1996). Imagination
964 inflation: Imagining a childhood event inflates confidence that it occurred. *Psychonomic*
965 *Bulletin and Review* *3*, 208–214.
- 966 3. Ferri, F., Venskus, A., Fotia, F., Cooke, J., and Romei, V. (2018). Higher proneness to
967 multisensory illusions is driven by reduced temporal sensitivity in people with high
968 schizotypal traits. *Consciousness and Cognition* *65*, 263–270.
- 969 4. Fenner, B., Cooper, N., Romei, V., and Hughes, G. (2020). Individual differences in
970 sensory integration predict differences in time perception and individual levels of schizotypy.
971 *Consciousness and Cognition* *84*, 102979.
- 972 5. Köther, U., Lincoln, T.M., and Moritz, S. (2018). Emotion perception and
973 overconfidence in errors under stress in psychosis. *Psychiatry Research* *270*, 981–991.
- 974 6. Klimesch, W., Sauseng, P., and Hanslmayr, S. (2007). EEG alpha oscillations: The
975 inhibition-timing hypothesis. *Brain Research Reviews* *53*, 63–88.
- 976 7. Mazaheri, A., and Jensen, O. (2010). Rhythmic pulsing: linking ongoing brain activity
977 with evoked responses. *Frontiers in Human Neuroscience* *4*, 1–13.
- 978 8. Palva, S., and Palva, J.M. (2007). New vistas for α -frequency band oscillations.
979 *Trends in Neurosciences* *30*, 150–158.
- 980 9. Samaha, J., Iemi, L., Haegens, S., and Busch, N.A. (2020). Spontaneous Brain
981 Oscillations and Perceptual Decision-Making. *Trends in Cognitive Sciences* *24*, 639–653.
- 982 10. Zazio, A., Schreiber, M., Miniussi, C., and Bortoletto, M. (2020). Modelling the
983 effects of ongoing alpha activity on visual perception: The oscillation-based probability of
984 response. *Neuroscience and Biobehavioral Reviews* *112*, 242–253.
- 985 11. Zoefel, B., and VanRullen, R. (2017). Oscillatory mechanisms of stimulus processing
986 and selection in the visual and auditory systems: State-of-the-art, speculations and
987 suggestions. *Frontiers in Neuroscience* *11*, 1–13.
- 988 12. VanRullen, R. (2016). Perceptual Cycles. *Trends in Cognitive Sciences* *20*, 723–735.
- 989 13. Wutz, A., and Melcher, D. (2014). The temporal window of individuation limits
990 visual capacity. *Frontiers in Psychology* *5*, 1–14.
- 991 14. Jensen, O., Gips, B., Bergmann, T.O., and Bonnefond, M. (2014). Temporal coding
992 organized by coupled alpha and gamma oscillations prioritize visual processing. *Trends in*
993 *Neurosciences* *37*, 357–369.
- 994 15. Busch, N.A., and VanRullen, R. (2010). Spontaneous EEG oscillations reveal periodic
995 sampling of visual attention. *Proceedings of the National Academy of Sciences* *107*, 16048–
996 16053.
- 997 16. Romei, V., Brodbeck, V., Michel, C., Amedi, A., Pascual-Leone, A., and Thut, G.
998 (2008). Spontaneous fluctuations in posterior α -band EEG activity reflect variability in
999 excitability of human visual areas. *Cerebral Cortex* *18*, 2010–2018.
- 1000 17. Benwell, C.S.Y., Tagliabue, C.F., Veniero, D., Cecere, R., Savazzi, S., and Thut, G.
1001 (2017). Pre-stimulus EEG power predicts conscious awareness but not objective visual
1002 performance. *Eneuro* *4*, ENEURO.0182-17.2017.
- 1003 18. Samaha, J., Iemi, L., and Postle, B.R. (2017). Prestimulus alpha-band power biases
1004 visual discrimination confidence, but not accuracy. *Consciousness and Cognition* *54*, 47–55.
- 1005 19. Iemi, X.L., Chaumon, M., Se, X., Crouzet, M., and Busch, X.N.A. (2017).
1006 Spontaneous Neural Oscillations Bias Perception by Modulating Baseline Excitability.

1007 Journal of Neuroscience 37, 807–819.

1008 20. Limbach, K., and Corballis, P.M. (2016). Prestimulus alpha power influences
1009 response criterion in a detection task. *Psychophysiology* 53, 1154–1164.

1010 21. Cecere, R., Rees, G., and Romei, V. (2015). Individual differences in alpha frequency
1011 drive crossmodal illusory perception. *Current Biology* 25, 231–235.

1012 22. Minami, S., and Amano, K. (2017). Illusory Jitter Perceived at the Frequency of
1013 Alpha Oscillations. *Current Biology* 27, 2344–2351.

1014 23. Samaha, J., and Postle, B.R. (2015). The Speed of Alpha-Band Oscillations Predicts
1015 the Temporal Resolution of Visual Perception. *Current Biology* 25, 2985–2990.

1016 24. Wutz, A., Melcher, D., and Samaha, J. (2018). Frequency modulation of neural
1017 oscillations according to visual task demands. *Proceedings of the National Academy of
1018 Sciences of the United States of America* 115, 1346–1351.

1019 25. Cooke, J., Poch, C., Gillmeister, H., Costantini, M., and Romei, V. (2019). Oscillatory
1020 Properties of Functional Connections Between Sensory Areas Mediate Cross-Modal Illusory
1021 Perception. *The Journal of neuroscience : the official journal of the Society for Neuroscience*
1022 39, 5711–5718.

1023 26. Migliorati, D., Zappasodi, F., Perrucci, M.G., Donno, B., Northoff, G., Romei, V.,
1024 and Costantini, M. (2020). Individual Alpha Frequency Predicts Perceived Visuotactile
1025 Simultaneity. *Journal of Cognitive Neuroscience* 32, 1–11.

1026 27. Mierau, A., Klimesch, W., and Lefebvre, J. (2017). State-dependent alpha peak
1027 frequency shifts: Experimental evidence, potential mechanisms and functional implications.
1028 *Neuroscience*.

1029 28. Green, D.M., and Swets, J.A. (1966). Signal detection theory and psychophysics. John
1030 Wiley, ed. (Oxford, England).

1031 29. Maniscalco, B., and Lau, H. (2012). A signal detection theoretic approach for
1032 estimating metacognitive sensitivity from confidence ratings. *Consciousness and Cognition*.

1033 30. Yeung, N., and Summerfield, C. (2012). Metacognition in human decision-making:
1034 confidence and error monitoring. *Philosophical Transactions of the Royal Society B:
1035 Biological Sciences* 367, 1310–1321.

1036 31. Murphy, P.R., Robertson, I.H., Harty, S., and O’Connell, R.G. (2015). Neural
1037 evidence accumulation persists after choice to inform metacognitive judgments. *eLife*, 1–23.

1038 32. Pleskac, T.J., and Busemeyer, J.R. (2010). Two-stage dynamic signal detection: A
1039 theory of choice, decision time, and confidence. *Psychological Review* 117, 864–901.

1040 33. Iemi, L., Busch, N.A., Laudini, A., Haegens, S., Samaha, J., Villringer, A., and
1041 Nikulin, V. V. (2019). Multiple mechanisms link prestimulus neural oscillations to sensory
1042 responses. *eLife* 8, 1–34.

1043 34. Romei, V., Thut, G., Mok, R.M., Schyns, P.G., and Driver, J. (2012). Causal
1044 implication by rhythmic transcranial magnetic stimulation of alpha frequency in feature-
1045 based local vs. global attention. *The European journal of neuroscience* 35, 968–974.

1046 35. Romei, V., Driver, J., Schyns, P.G., and Thut, G. (2011). Rhythmic TMS over Parietal
1047 Cortex Links Distinct Brain Frequencies to Global versus Local Visual Processing. *Current
1048 Biology* 21, 334–337.

1049 36. Romei, V., Thut, G., and Silvanto, J. (2016). Information-Based Approaches of
1050 Noninvasive Transcranial Brain Stimulation. *Trends in Neurosciences* 39, 782–795.

1051 37. Thut, G., Veniero, D., Romei, V., Miniussi, C., Schyns, P., and Gross, J. (2011).
1052 Rhythmic TMS causes local entrainment of natural oscillatory signatures. *Current Biology*
1053 21, 1176–1185.

1054 38. Helfrich, R.F., Schneider, T.R., Rach, S., Trautmann-Lengsfeld, S.A., Engel, A.K.,
1055 and Herrmann, C.S. (2014). Entrainment of brain oscillations by transcranial alternating
1056 current stimulation. *Current Biology* 24, 333–339.

- 1057 39. Thut, G., Bergmann, T.O., Fröhlich, F., Soekadar, S.R., Brittain, J.S., Valero-Cabré,
1058 A., Sack, A.T., Miniussi, C., Antal, A., Siebner, H.R., et al. (2017). Guiding transcranial
1059 brain stimulation by EEG/MEG to interact with ongoing brain activity and associated
1060 functions: A position paper. *Clinical Neurophysiology* 128, 843–857.
- 1061 40. Veniero, D., Vossen, A., Gross, J., and Thut, G. (2015). Lasting EEG/MEG
1062 aftereffects of rhythmic transcranial brain stimulation: Level of control over oscillatory
1063 network activity. *Frontiers in Cellular Neuroscience* 9, 1–17.
- 1064 41. Romei, V., Bauer, M., Brooks, J.L., Economides, M., Penny, W., Thut, G., Driver, J.,
1065 and Bestmann, S. (2016). Causal evidence that intrinsic beta-frequency is relevant for
1066 enhanced signal propagation in the motor system as shown through rhythmic TMS.
1067 *NeuroImage* 126, 120–130.
- 1068 42. Ergenoglu, T., Demiralp, T., Bayraktaroglu, Z., Ergen, M., Beydagi, H., and Uresin,
1069 Y. (2004). Alpha rhythm of the EEG modulates visual detection performance in humans.
1070 *Cognitive Brain Research* 20, 376–383.
- 1071 43. van Dijk, H., Schoffelen, J.-M., Oostenveld, R., and Jensen, O. (2008). Prestimulus
1072 Oscillatory Activity in the Alpha Band Predicts Visual Discrimination Ability. *Journal of*
1073 *Neuroscience* 28, 1816–1823.
- 1074 44. Roberts, D.M., Fedota, J.R., Buzzell, G.A., Parasuraman, R., and McDonald, C.G.
1075 (2014). Prestimulus Oscillations in the Alpha Band of the EEG Are Modulated by the
1076 Difficulty of Feature Discrimination and Predict Activation of a Sensory Discrimination
1077 Process. *Journal of Cognitive Neuroscience* 26, 1615–1628.
- 1078 45. Baumgarten, T.J., Schnitzler, A., and Lange, J. (2016). Prestimulus Alpha Power
1079 Influences Tactile Temporal Perceptual Discrimination and Confidence in Decisions.
1080 *Cerebral Cortex* 26, 891–903.
- 1081 46. Iemi, L., and Busch, N.A. (2018). Moment-to-Moment Fluctuations in Neuronal
1082 Excitability Bias Subjective Perception Rather than Strategic Decision-Making. *Eneuro* 5, 1–
1083 13.
- 1084 47. Weisz, N., Lüchinger, C., Thut, G., and Müller, N. (2014). Effects of individual alpha
1085 rTMS applied to the auditory cortex and its implications for the treatment of chronic tinnitus.
1086 *Hum Brain Mapp* 35, 14–29.
- 1087 48. Hanslmayr, S., Matuschek, J., and Fellner, M.-C. (2014). Entrainment of prefrontal
1088 beta oscillations induces an endogenous echo and impairs memory formation. *Curr Biol* 24,
1089 904–909.
- 1090 49. Varela, F.J., Toro, A., Roy John, E., and Schwartz, E.L. (1981). Perceptual framing
1091 and cortical alpha rhythm. *Neuropsychologia* 19, 675–686.
- 1092 50. Mathewson, K.E., Gratton, G., Fabiani, M., Beck, D.M., and Ro, T. (2009). To See or
1093 Not to See: Prestimulus Phase Predicts Visual Awareness. *Journal of Neuroscience* 29, 2725–
1094 2732.
- 1095 51. Dugué, L., Marque, P., and VanRullen, R. (2011). The phase of ongoing oscillations
1096 mediates the causal relation between brain excitation and visual perception. *Journal of*
1097 *Neuroscience* 31, 11889–11893.
- 1098 52. Busch, N.A., Dubois, J., and VanRullen, R. (2009). The phase of ongoing EEG
1099 oscillations predicts visual perception. *Journal of Neuroscience* 29, 7869–7876.
- 1100 53. Haegens, S., Nacher, V., Luna, R., Romo, R., and Jensen, O. (2011). α -Oscillations in
1101 the monkey sensorimotor network influence discrimination performance by rhythmical
1102 inhibition of neuronal spiking. *PNAS* 108, 19377–19382.
- 1103 54. Navajas, J., Bahrami, B., and Latham, P.E. (2016). Post-decisional accounts of biases
1104 in confidence. *Current Opinion in Behavioral Sciences* 11, 55–60.
- 1105 55. Fleming, S.M., and Daw, N.D. (2017). Self-Evaluation of Decision-Making: A
1106 General Bayesian Framework for Metacognitive Computation. *Psychol Rev* 124, 91–114.

- 1107 56. Pereira, M., Faivre, N., Iturrate, I., Wirthlin, M., Serafini, L., Martin, S., Desvachez,
1108 A., Blanke, O., Van De Ville, D., and Millán, J. del R. (2020). Disentangling the origins of
1109 confidence in speeded perceptual judgments through multimodal imaging. *Proc Natl Acad*
1110 *Sci USA* *117*, 8382–8390.
- 1111 57. Posner, M.I., Snyder, C.R., and Davidson, B.J. (1980). Attention and the detection of
1112 signals. *Journal of Experimental Psychology: General* *109*, 160–174.
- 1113 58. Fan, J., McCandliss, B.D., Sommer, T., Raz, A., and Posner, M.I. (2002). Testing the
1114 Efficiency and Independence of Attentional Networks. *Journal of Cognitive Neuroscience* *14*,
1115 340–347.
- 1116 59. Thut, G., Nietzel, A., Brandt, S., and Pascual-Leone, A. (2006). Alpha Band
1117 Electroencephalographic Activity over Occipital Cortex Indexes Visuospatial Attention Bias
1118 and Predicts Visual Target Detection. *Journal of Neuroscience* *13*, 9494–9502.
- 1119 60. Rihs, T.A., Michel, C.M., and Thut, G. (2007). Mechanisms of selective inhibition in
1120 visual spatial attention are indexed by α -band EEG synchronization. *European Journal of*
1121 *Neuroscience* *25*, 603–610.
- 1122 61. Tarasi, L., Trajkovic, J., Diciotti, S., di Pellegrino, G., Ferri, F., Ursino, M., and
1123 Romei, V. (2021). Predictive waves in the autism-schizophrenia continuum: A novel
1124 biobehavioral model. *Neurosci Biobehav Rev* *132*, 1–22.
- 1125 62. Haegens, S., Cousijn, H., Wallis, G., Harrison, P.J., and Nobre, A.C. (2014). Inter-
1126 and intra-individual variability in alpha peak frequency. *NeuroImage*.
- 1127 63. Hülzdünker, T., Mierau, A., and Strüder, H.K. (2016). Higher balance task demands
1128 are associated with an increase in individual alpha peak frequency. *Frontiers in Human*
1129 *Neuroscience*.
- 1130 64. Maurer, U., Brem, S., Liechti, M., Maurizio, S., Michels, L., and Brandeis, D. (2014).
1131 Frontal Midline Theta Reflects Individual Task Performance in a Working Memory Task.
1132 *Brain Topography*.
- 1133 65. Samaha, J., Bauer, P., Cimaroli, S., and Postle, B.R. (2015). Top-down control of the
1134 phase of alpha-band oscillations as a mechanism for temporal prediction. *Proceedings of the*
1135 *National Academy of Sciences of the United States of America* *112*, 8439–8444.
- 1136 66. Benwell, C.S.Y., Coldea, A., Harvey, M., and Thut, G. (2021). Low pre-stimulus
1137 EEG alpha power amplifies visual awareness but not visual sensitivity. *European Journal of*
1138 *Neuroscience*, 1–16.
- 1139 67. Romei, V., Gross, J., and Thut, G. (2010). On the role of prestimulus alpha rhythms
1140 over occipito-parietal areas in visual input regulation: Correlation or causation? *Journal of*
1141 *Neuroscience* *30*, 8692–8697.
- 1142 68. Albouy, P., Weiss, A., Baillet, S., and Zatorre, R.J. (2017). Selective Entrainment of
1143 Theta Oscillations in the Dorsal Stream Causally Enhances Auditory Working Memory
1144 Performance. *Neuron* *94*, 193-206.e5.
- 1145 69. Vernet, M., Stengel, C., Quentin, R., Amengual, J.L., and Valero-Cabré, A. (2019).
1146 Entrainment of local synchrony reveals a causal role for high-beta right frontal oscillations in
1147 human visual consciousness. *Scientific Reports* *9*, 1–15.
- 1148 70. Sauseng, P., Klimesch, W., Heise, K.F., Gruber, W.R., Holz, E., Karim, A.A.,
1149 Glennon, M., Gerloff, C., Birbaumer, N., and Hummel, F.C. (2009). Brain Oscillatory
1150 Substrates of Visual Short-Term Memory Capacity. *Current Biology* *19*, 1846–1852.
- 1151 71. Chanes, L., Quentin, R., Tallon-Baudry, C., and Valero-Cabré, A. (2013). Causal
1152 frequency-specific contributions of frontal spatiotemporal patterns induced by non-invasive
1153 neurostimulation to human visual performance. *Journal of Neuroscience* *33*, 5000–5005.
- 1154 72. De Martino, B., Fleming, S.M., Garrett, N., and Dolan, R.J. (2013). Confidence in
1155 value-based choice. *Nature neuroscience* *16*, 105–110.
- 1156 73. Wolinski, N., Cooper, N.R., Sauseng, P., and Romei, V. (2018). The speed of parietal

1157 theta frequency drives visuospatial working memory capacity. *PLoS Biology*.

1158 74. Bestmann, S., Ruff, C.C., Blakemore, C., Driver, J., and Thilo, K. V (2007). Spatial
1159 Attention Changes Excitability of Human Visual Cortex to Direct Stimulation. *Current*
1160 *Biology* *17*, 134–139.

1161 75. Cattaneo, Z., Silvanto, J., Battelli, L., and Pascual-Leone, A. (2009). The mental
1162 number line modulates visual cortical excitability. *Neurosci Lett* *462*, 253–256.

1163 76. Silvanto, J., and Muggleton, N.G. (2008). A novel approach for enhancing the
1164 functional specificity of TMS: Revealing the properties of distinct neural populations within
1165 the stimulated region. *Clinical Neurophysiology* *119*, 124.

1166 77. Mevorach, C., Humphreys, G.W., and Shalev, L. (2006). Opposite biases in salience-
1167 based selection for the left and right posterior parietal cortex. *Nature Neuroscience*.

1168 78. Pitcher, D., Walsh, V., Yovel, G., and Duchaine, B. (2007). TMS Evidence for the
1169 Involvement of the Right Occipital Face Area in Early Face Processing. *Current Biology* *17*,
1170 1568–1573.

1171 79. Silvanto, J., Lavie, N., and Walsh, V. (2005). Double dissociation of V1 and V5/MT
1172 activity in visual awareness. *Cerebral Cortex* *15*, 1736–1741.

1173 80. Bolognini, N., Senna, I., Maravita, A., Pascual-Leone, A., and Merabet, L.B. (2010).
1174 Auditory enhancement of visual phosphene perception: The effect of temporal and spatial
1175 factors and of stimulus intensity. *Neuroscience Letters*.

1176 81. Gerwig, M., Kastrup, O., Meyer, B.U., and Niehaus, L. (2003). Evaluation of cortical
1177 excitability by motor and phosphene thresholds in transcranial magnetic stimulation. *Journal*
1178 *of the Neurological Sciences*.

1179 82. Romei, V., Murray, M.M., Cappe, C., and Thut, G. (2009). Preperceptual and
1180 Stimulus-Selective Enhancement of Low-Level Human Visual Cortex Excitability by
1181 Sounds. *Current Biology* *19*, 1799–1805.

1182 83. Romei, V., Murray, M.M., Merabet, L.B., and Thut, G. (2007). Occipital transcranial
1183 magnetic stimulation has opposing effects on visual and auditory stimulus detection:
1184 Implications for multisensory interactions. *Journal of Neuroscience* *27*, 11465–11472.

1185 84. Romei, V., Rihs, T., Brodbeck, V., and Thut, G. (2008). Resting
1186 electroencephalogram alpha-power over posterior sites indexes baseline visual cortex
1187 excitability. *NeuroReport* *19*, 203–208.

1188 85. Rossi, S., Hallett, M., Rossini, P.M., and Pascual-Leone, A. (2009). Safety, ethical
1189 considerations, and application guidelines for the use of transcranial magnetic stimulation in
1190 clinical practice and research. *Clin Neurophysiol* *120*, 2008–2039.

1191 86. Delorme, A., and Makeig, S. (2004). EEGLAB: An open source toolbox for analysis
1192 of single-trial EEG dynamics including independent component analysis. *Journal of*
1193 *Neuroscience Methods*.

1194 87. Gratton, G., Coles, M.G.H., and Donchin, E. (1983). A new method for off-line
1195 removal of ocular artifact. *Electroencephalography and Clinical Neurophysiology* *55*, 468–
1196 484.

1197 88. Cavanagh, J.F., Figueroa, C.M., Cohen, M.X., and Frank, M.J. (2012). Frontal theta
1198 reflects uncertainty and unexpectedness during exploration and exploitation. *Cerebral Cortex*
1199 *22*, 2575–2586.

1200 89. Di Gregorio, F., Maier, M.E., and Steinhauser, M. (2018). Errors can elicit an error
1201 positivity in the absence of an error negativity: Evidence for independent systems of human
1202 error monitoring. *NeuroImage* *172*, 427–436.

1203 90. Barrett, A.B., Dienes, Z., and Seth, A.K. (2013). Measures of metacognition on
1204 signal-detection theoretic models. *Psychological Methods* *18*, 535–552.

1205 91. Rogasch, N.C., Sullivan, C., Thomson, R.H., Rose, N.S., Bailey, N.W., Fitzgerald,
1206 P.B., Farzan, F., and Hernandez-Pavon, J.C. (2017). Analysing concurrent transcranial

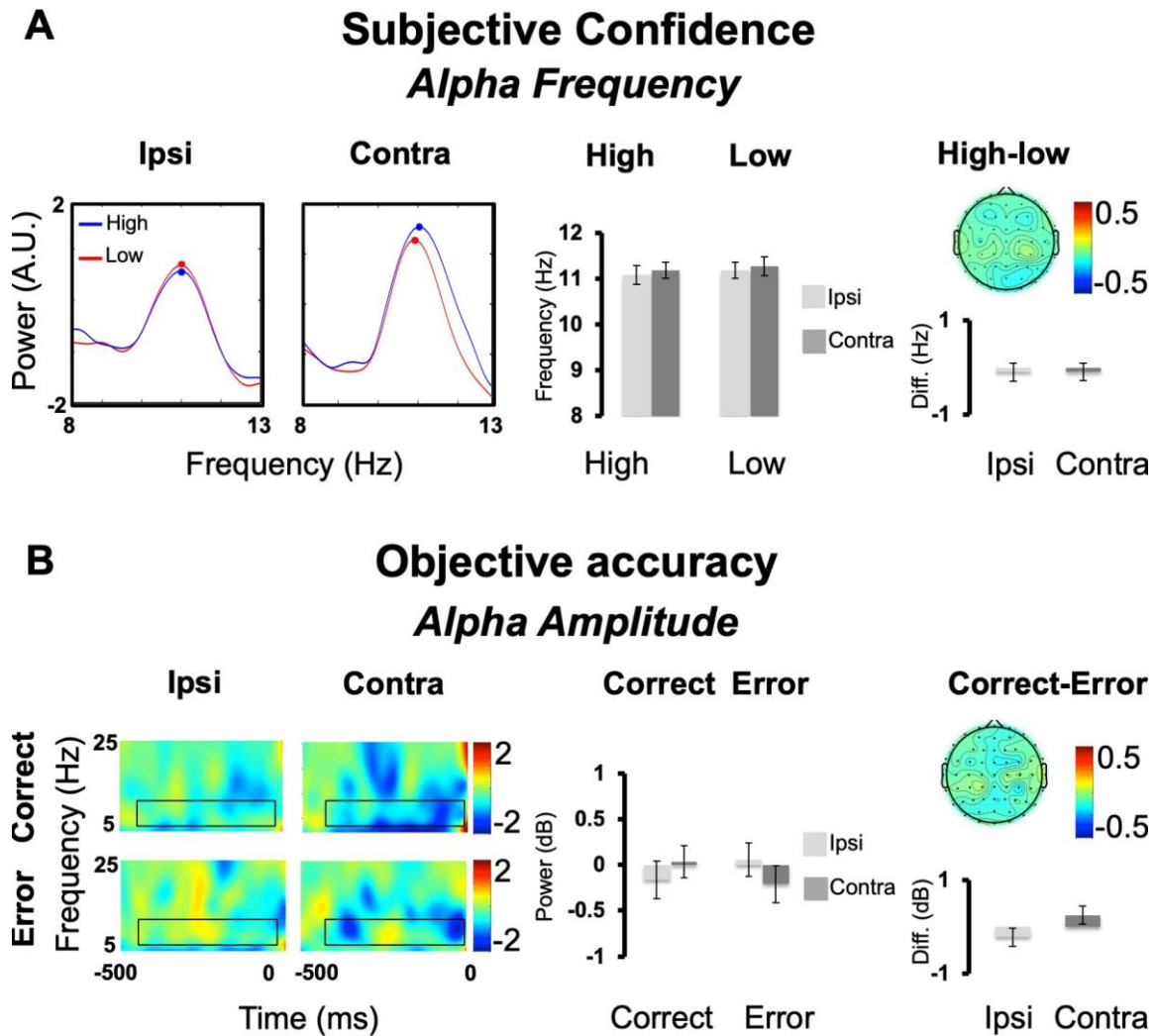
1207 magnetic stimulation and electroencephalographic data: A review and introduction to the
1208 open-source TESA software. NeuroImage.

1209
1210
1211
1212
1213
1214
1215
1216
1217
1218
1219
1220
1221
1222
1223
1224
1225
1226
1227
1228
1229
1230
1231
1232
1233
1234
1235
1236
1237
1238
1239
1240
1241
1242
1243
1244
1245
1246
1247
1248
1249
1250
1251
1252
1253
1254
1255
1256

1257

Control Analyses and Results

1258



1259

1260

1261

1262

1263

1264

1265

1266

1267

1268

1269

1270

1271

1272

1273

1274

1275

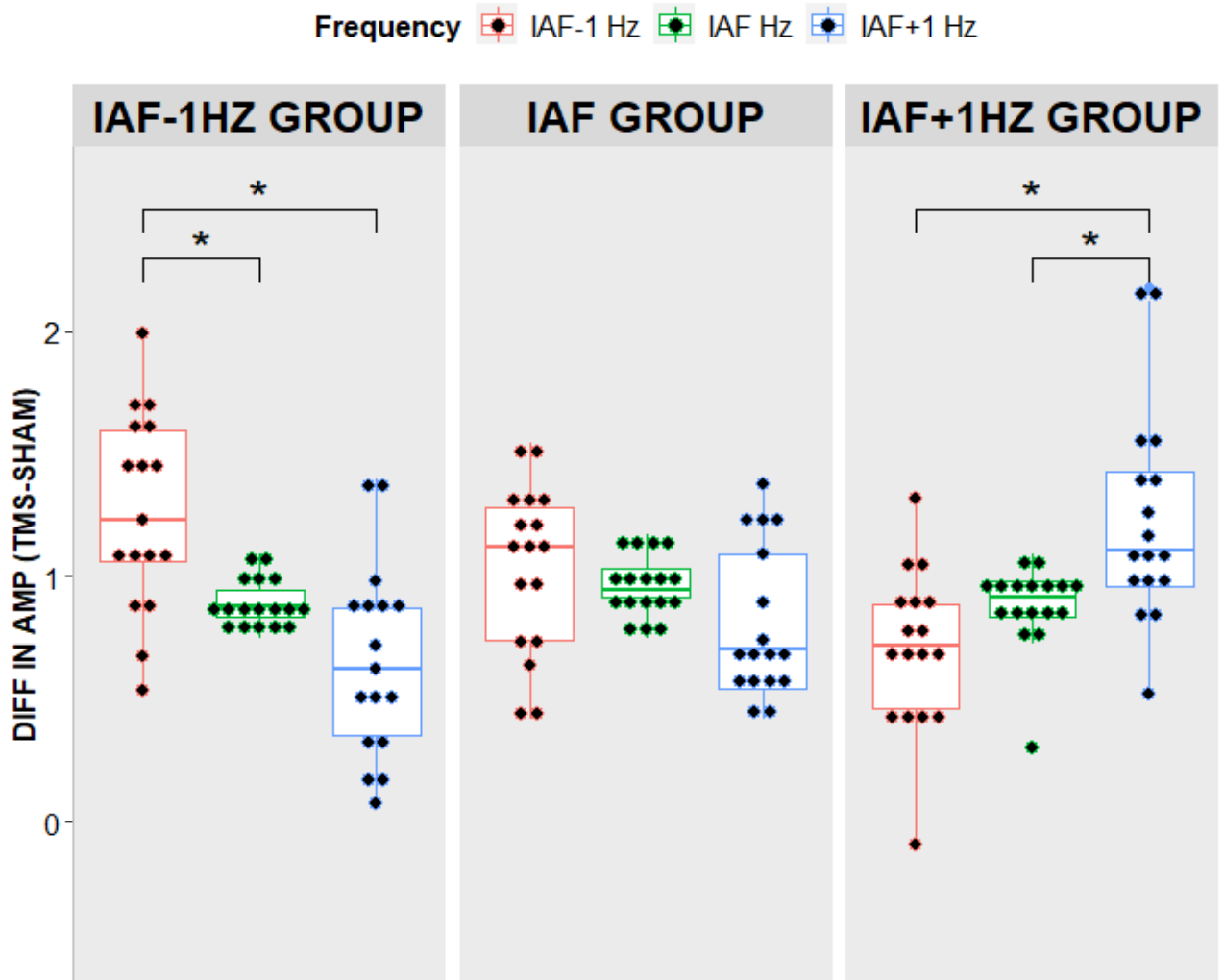
1276

1277

1278

Figure S1. Results Experiment 1: Alpha-frequency and -amplitude in accuracy and confidence, related to Figure 2. A. Subjective Confidence. Averaged Alpha-frequency is represented as the z-scored mean power ($10 \cdot \log_{10}[\mu\text{V}^2/\text{Hz}]$) spectrum in the cue-stimulus time period for the contralateral and the ipsilateral electrodes and for Low and High confident trials within the alpha band. Bar graphs are reported for Low and High confident trials and for the difference in High-Low. Topography represents the difference High-Low (electrodes are flipped to represent contralateral activity in the right-hand side and ipsilateral activity in the left-hand side). No statistical effects reached significance (all $F_s(1,23) < 0.47$; $p_s > .501$; $\eta_{ps} < .021$), suggesting that alpha-frequency has no role in determining one individual confidence on their response. B. Objective Accuracy. Alpha-Amplitude is reported as time-frequency plots for the contralateral and the ipsilateral electrodes and for Correct and Error trials. Black boxes denote regions of statistical analyses (alpha band 7-13Hz). Bar graphs are reported for Correct and Error trials and for the difference in Correct-Error. Topography represents the difference Correct-Error (electrodes are flipped to have contralateral activity in the right-hand side and ipsilateral activity in the left-hand side). No statistical effects reached significance (all $F_s(1,23) < 2.133$;

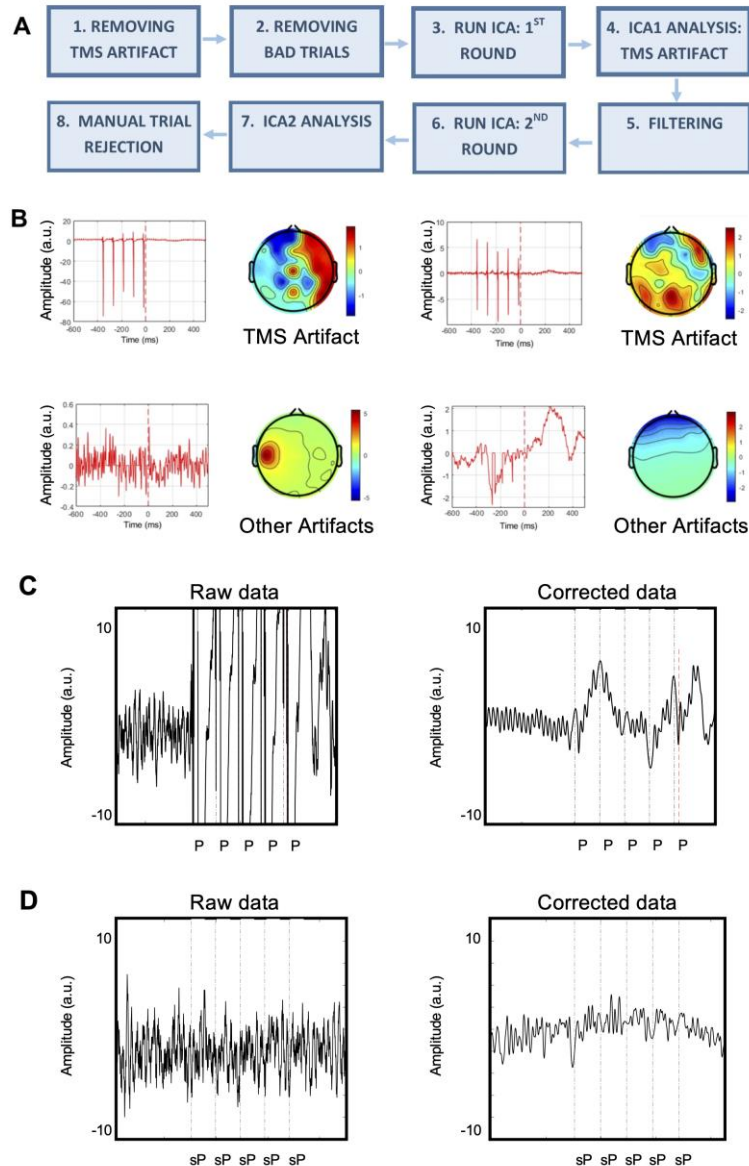
1279 ps>.158; η_{ps} <.085), suggesting that alpha-amplitude has no role in determining
 1280 objective accuracy. Error bars represent standard error of the mean
 1281 A.U.=arbitrary units; Diff=difference; μ v=microvolt; Hz=Hertz; ms=milliseconds;
 1282 dB=decibel.
 1283



1284
 1285
 1286 **Figure S2. Results Experiment 2: Differences in alpha-amplitude across**
 1287 **frequencies, Related to Figure 3.** Box plots of differences in averaged alpha-
 1288 amplitude between Active and Sham stimulation blocks for three experimental
 1289 groups (IAF±1 and IAF groups) and for different frequencies (IAF1±Hz, and IAF
 1290 frequencies). Horizontal lines represent the median value, while vertical lines
 1291 represent the 25th and 75th percentile. Two-tailed t-tests are reported (*p<.05),
 1292 showing highest differences between Active and Sham stimulation at the stimulated
 1293 frequency both in the IAF-1 Hz and IAF+1 Hz groups. The effects gradually and
 1294 significantly decreased at different alpha frequencies: all t s>2.45, all p s<.026, all
 1295 d s>0.34. In the IAF group, there were no significant differences between flanker
 1296 (higher and lower) alpha frequencies ($F(2,32)=2.289$; $p=.150$; $\eta_p^2=.12$), speaking in
 1297 favor of a broadband entrainment effect in the alpha band for this group.
 1298

1299 Control Methods

1300 Experiment 2 and 3



1301 **Figure S3. TMS artefact correction procedure, related to STAR Methods.** A.
1302 EEG data processing workflow and pipeline for Experiments 2 and 3. B. Examples of
1303 artefact components removed in the first (TMS artefacts, upper row) and second
1304 (lower row) ICA analyses C. Effects of artefact rejection procedure on an active TMS
1305 condition. One second epoch of one participant before (Raw data) and after
1306 (Corrected data) the correction procedure. Dashed lines reflect Pre-stimulus TMS
1307 pulses (P) D. Effects of artefact rejection procedure on a TMS-artefact free signal.
1308 The procedure was applied to ensure that any effect we have observed could not be
1309 alternatively explained by a spurious effect of the cleaning protocol adopted. One
1310 second epoch of one participant before (Raw data) and after (Corrected data)
1311 correction procedure. It can be noticed that the artefact-removal procedure per se
1312 does not alter the underlying signal, confirming that the artefact-rejection procedure
1313

1314 per se is not accountable for the modulation of the oscillatory activity. Dashed lines
1315 reflect simulated pulses (sP). ICA=Independent Components Analyses,
1316 A.U.=Arbitrary Units, ms=millisecond.
1317